Communications Earth & Environment https://doi.org/10.1038/s43247-026-03789-1

Article in Press

Functional and genomic potential of microbial communities in TNT-contaminated sediments at a historical submarine wreck

Received: 14 October 2025

Accepted: 29 June 2026

Published online: 11 July 2026

Cite this article as: Vuerstaek, R., Heyse, J., Lacoere, T. *et al.* Functional and genomic potential of microbial communities in TNT-contaminated sediments at a historical submarine wreck. *Commun Earth Environ* (2026). https://doi.org/10.1038/s43247-026-03789-1

Rune Vuerstaek, Jasmine Heyse, Tim Lacoere, Lillian Tabea Hannah Buenning, Maarten De Rijcke, Edmund Maser, Katrine Juul Andresen, Nico Boon & Kankana Kundu

Functional and genomic potential of microbial communities in TNT-contaminated sediments at a historical submarine wreck

Rune Vuerstaek[1,2], Jasmine Heyse[1], Tim Lacoere[1,2], Lillian Tabea Hannah Buenning[4], Maarten De Rijcke[5], Edmund Maser[4], Katrine Juul Andresen[3], Nico Boon[1,2], Kankana Kundu[1.2]*

[1]Center for Microbial Ecology and Technology (CMET), 9000 Ghent, Belgium

[2]Centre for Advanced Process Technology for Urban Resource recovery (CAPTURE), Ghent, Belgium

[3]Department of Geoscience, Aarhus University
Høegh-Guldbergs Gade 2, 8000 Aarhus C, Denmark

[4]Institute for Toxicology and Pharmacology for Natural Scientists, University Medical School Schleswig-Holstein, Campus Kiel, Brunswiker Strasse 10, 24105 Kiel, Germany

[5]Flanders Marine Institute (VLIZ), InnovOcean Campus, Jacobsenstraat 1, 8400 Ostend, Belgium

Corresponding Author
*Center for Microbial Ecology and Technology (CMET), Faculty of Bioscience Engineering, Ghent University, Frieda Saeysstraat 1, 9052 Gent, Belgium, kankana.kundu@ugent.be

Abstract

Unexploded ordnance from World Wars I and II continues to release 2,4,6-trinitrotoluene into marine sediments, yet microbial responses to this chronic contamination remain poorly understood. Here, we characterize the taxonomic and functional potential of sediment microbiomes at the historical submarine wreck UC-30 in the North Sea, combining 16S rRNA amplicon sequencing, shotgun metagenomics, and targeted GC-MS/MS analysis with a parallel aerobic laboratory enrichment. Minewell sediments showed distinct community shifts, with enrichment of Proteobacteria, notably *Haliaceae* and *Rhodobacteraceae*, alongside increased representation of oxidoreductases and stress-related enzyme classes, including glutathione S-transferases. Genes associated with TNT transformation, including Old Yellow Enzymes and nitroreductases, were modestly enriched in situ. The laboratory enrichment confirmed TNT removal and presence of N-ethylmaleimide reductase, an Old Yellow Enzyme implicated in TNT transformation. Functional and taxonomic parallels between field and enrichment communities indicate shared adaptive capacities under TNT exposure, positioning contaminated marine microbiomes as reservoirs of bioremediation potential.

1. Introduction

The global ocean harbors extraordinary microbial diversity, characterized by remarkable metabolic flexibility and essential roles in biogeochemical cycling, energy transfer, and ecosystem stability[1,2]. Despite extensive sequencing efforts, a large fraction of marine microbial diversity still remains taxonomically and functionally unresolved, with many genomes lacking assignment to known taxa[3]. Meanwhile, anthropogenic chemical pollutants are increasingly infiltrating marine environments, posing significant threats to ecosystem integrity and biological functioning[4]. The current situation creates an opportunity to explore the inherent capacity of indigenous marine microbiomes to detect, transform, and degrade environmental contaminants. Shaped by long-term evolutionary pressures, marine microorganisms have developed specialized enzymatic pathways and adaptive mechanisms that could offer natural solutions to mitigate human-induced pollution challenges.

Marine pollution includes hydrocarbons, plastics, heavy metals, and a wide range of industrial chemicals, but residues from dumped or sunken munitions are an increasingly recognized and persistent source of chemical stress in both coastal and deep-sea- ecosystems[5,6]. Between 1917 and 1970, up to 1.6 million tons of munitions were dumped or lost in the northern European seas, with hundreds of additional vessels carrying munitions sinking during wartime[7]. As the metal casings of these dumped munitions corrode, they slowly release explosive compounds, most notably 2,4,6-trinitrotoluene (TNT), into surrounding sediments and bottom waters, creating chronic contamination hotspots. Once released, TNT undergoes both abiotic (*e.g.,*

photolysis, reduction by reduced minerals, and chemical hydrolysis) and biotic transformation, producing a suite of derivatives including 2-hydroxylamino-4,6-dinitrotoluene (2-HADNT), 4-hydroxylamino-2,6-dinitrotoluene (4-HADNT), 2-amino-4,6-dinitrotoluene (2-ADNT), 4-amino-2,6-dinitrotoluene (4-ADNT), and 2,4-diamino-6-nitrotoluene (2,4-DANT)[8,9]. Among these, ADNTs are widely used indicators of biotic TNT transformation in sediment environments, where microbial reductive activity is the primary driver of their accumulation (Supplementary Figure 1). TNT and its metabolites can accumulate in benthic habitats, where they have been shown to exert sublethal and chronic effects on sediment dwelling organisms, even at low environmental concentrations[10,11]. Their uptake by invertebrates and fish raises concerns surrounding trophic transfer and potential human exposure through seafood consumption[12].

Localized marine TNT impact areas provide a powerful model for examining how environmental microbiomes respond to chemical stress. Although most mechanistic insights come from terrestrial systems, it is well established that microorganisms can transform TNT's recalcitrant, trinitrosubstituted structure through reductive pathways involving Type I nitroreductases- and Old Yellow Enzymes (OYEs) to products such as HADNTs and ADNTs[13,14]. Similar TNT transformation has also been demonstrated in marine isolates[15]. Despite these mechanistic insights, it is still unclear how chronic munition exposure shapes entire microbial communities *in situ* or whether contaminated environments select for taxa with enhanced transformation potential. Shallow-sea munition dump sites offer a unique opportunity to address this gap. Corroding explosives create stable contamination gradients that impose long-term selective pressure on benthic microbiomes, potentially enriching for microorganisms with specialized functional

traits relevant to contaminant transformation[16]. Resolving these community-level responses is essential for uncovering the largely unexplored metabolic potential of marine sediments exposed to persistent chemical stress.

We investigated the microbiome associated with UC-30, a German Type UC II minelaying submarine that sank near Horns Reef in the Danish North Sea in 1917 (23 m depth). The wreck contains six minewells that represent a very rare opportunity to study leaking munitions in a site that is both accessible and spatially contained, where corrosion has created localized TNT-impacted areas. These sediments reached concentrations up to 8.9 μg kg^{-1}, among the highest reported in situ[16–18]. Sediments from minewells and adjacent seafloor reference sites were analyzed using 16S rRNA gene sequencing and shotgun metagenomics to characterize taxonomic composition and functional gene distributions across contamination gradients. Seafloor reference samples were positioned immediately adjacent to the minewells to ensure that comparisons reflected the local TNT concentration gradient rather than larger-scale environmental differences. Due to its low Henry's Law constant and limited solubility in seawater, TNT has very low volatility, dissolves slowly, and is strongly retained in sediments[19]. Consequently, minewells act as localized, persistent contamination sources, making them well suited for studying long-term microbial exposure to explosive compounds. To complement the in situ data, we conducted an aerobic TNT enrichment experiment using 80 mg L^{-1} of TNT, a concentration chosen to impose strong contaminant pressure while remaining below TNT's solubility limit (~130 mg L^{-1}). This allowed us to identify resistant taxa and their associated functional traits, providing a controlled comparison to environmental communities. Although enrichment conditions do not replicate the full complexity of the

minewell environment, parallels between the two systems can still reveal microbial lineages and functions that are relevant, even if not exclusively causal, to TNT exposure. In parallel, we aimed to obtain preliminary chemical evidence of TNT transformation; however, detailed chemical characterization was not a priority of this study.

We hypothesized that long-term exposure to leaking munitions has shaped the minewell microbiome, enriching for taxa and functional traits associated with TNT tolerance and transformation, and that these communities would exhibit taxonomic and functional patterns that mirror those observed in the enrichment cultures. Together, these approaches provide one of the first comprehensive characterizations of a marine microbiome under chronic explosive contamination and establish a framework for evaluating microbial functional potential in polluted marine sediments.

2. Results and Discussion

2.1 TNT spreads to the surrounding sediments

Chemical analysis revealed markedly elevated TNT concentrations within the minewells compared to the surrounding seafloor (Table 1). TNT levels in minewells ranged from 0.144 to 8.939 µg/kg, which is one of the highest measured TNT concentrations found in the marine environment[16–18]. Surrounding seafloor sediments contained only ~10 ng/kg. TNT metabolites showed a similar pattern, with maxima of 3.454 µg/kg (4-ADNT) and 2.308 µg/kg (2-ADNT) in minewells, compared to much lower concentrations in underlying seafloor sediments (0.179 and 0.112 µg/kg, respectively).

The consistent presence of 4-ADNT and 2-ADNT indicates ongoing transformation of TNT into reduced intermediates. While abiotic processes, particularly photolytic degradation, can drive TNT attenuation in illuminated marine waters[9,41,42], it has been postulated that bacterial mineralization occurs concurrently and that photochemical reactions may even enhance microbial activity[41]. The accumulation of ADNTs indicates active microbial TNT reduction, consistent with the degradation observed in our enrichment experiment (Section 3.7). This interpretation is consistent with previous findings showing that biotic processes contribute measurably to TNT removal in marine sediments, where particle surfaces facilitate microbial attachment and enhance sorption-driven biodegradation[43].

The predominance of 4-ADNT over 2-ADNT, and its higher concentrations relative to TNT in most samples (except UC30 M2 and UC30 M3), suggests preferential transformation via nitroreduction to 4-ADNT, a pathway documented in several TNT-degrading bacterial taxa[44,45]. Variation in TNT and metabolite concentrations among minewell samples may reflect differences in munition corrosion rates and thus heterogeneous exposure durations for the associated microbiomes, though other factors such as localized differences in geochemical conditions cannot be excluded (Supplementary Figure 2). Concentrations of 2,4-DNT and 1,3-DNB were frequently below detection limits (Section 2.2). As these compounds are manufacturing byproducts rather than TNT transformation products, their presence or absence reflects the original munition composition and is not necessarily indicative of degradation activity (Supplementary Figure 1).

2.2 The microbial community structure differs between minewells and the seafloor

Microbial community composition differed markedly between minewell and seafloor samples. Beta-diversity analysis revealed a clear and statistically significant separation between minewell and seafloor communities (PERMANOVA, R^2=0.17, p = 0.001; Figure 1B), with homogeneous within-group dispersion confirmed (betadisper, F = 0.161, p = 0.701), indicating that this separation reflects genuine differences in community composition. No significant differences were observed in alpha-diversity between environments, as assessed by Richness (number of observed taxa), Shannon index (richness and evenness), and Simpson index (dominance-sensitive diversity) (Mann–Whitney test, p > 0.05; Figure 1A).

Although alpha-diversity metrics did not differ significantly between environments, minewell samples generally showed lower richness and diversity than seafloor samples across all indices (Figure 1A). This trend suggests a reduction in within-sample diversity that may be obscured by limited statistical power and the high degree of heterogeneity among minewells. Reduced alpha diversity in minewells is ecologically expected. These wells contain relatively higher contaminant levels, as shown by the elevated TNT concentrations measured in this study (Table 1). Toxic compounds act as environmental filters by imposing selective pressures that favor contaminant-tolerant or specialized taxa[46]. Consistent with this interpretation, reductions in alpha diversity in response to energetic compounds, including TNT, have been reported in contaminated soils and sediments[47–49].

Minewells represent relatively isolated microhabitats that can promote localized accumulation of contaminants, in contrast to the more continuous and interconnected seafloor environment. Despite rarefaction analyses indicating sufficient sequencing depth (Supplementary Figure 3), alpha-diversity indices varied among minewell samples. Such heterogeneity is common in environmental microbial communities and may reflect the inherently dynamic and stochastic nature of microbial community assembly and succession. While differences in contamination history, contaminant load, and exposure duration could contribute to this variability, these factors were not directly assessed in the present study. Given the close spatial proximity of the seafloor and minewell sampling locations, large-scale environmental parameters such as temperature and sediment type are less likely to account for the observed differences. Nevertheless, the overall separation between contaminated and surrounding seafloor communities indicates a substantial restructuring of community composition, consistent with observations from other contaminated soil and sediment systems where toxic compounds influence microbial assemblages[50].

2.3 Proteobacteria dominate community shifts in minewells

Proteobacteria accounted for a substantial share of the community restructuring observed in minewells, with *Rhodobacteraceae* and *Haliaceae* contributing through both increased abundance and elevated taxonomic diversity. Differential abundance analysis (DESeq2, Benjamini–Hochberg correction, *FDR* < 0.1) identified 11 ASVs significantly enriched in minewells, with 6 ASVs (54.5%) classified within Proteobacteria (Figure 2D). Proteobacteria reached a significantly higher relative abundance in minewell samples (27.5% ± 1.6%) compared to seafloor sediments (22.7% ± 1.0%; Mann–Whitney test, p

= 8.23 × 10^{-5}; Figure 2B), representing the most abundant phylum in minewell communities (Supplementary Figure 4). Within Proteobacteria, both *Rhodobacteraceae* (6.4% ± 2.1% vs. 3.4% ± 0.7%; Mann–Whitney test; p = 0.011) and *Haliaceae* (3.5% ± 0.4% vs. 2.3% ± 0.4%; Mann–Whitney test; p = 0.003) showed enrichment in minewells relative to seafloor samples (Figure 2B). At the class level, Alphaproteobacteria (13.0% ± 2.48% vs. 8.8% ± 0.74%; Mann–Whitney test, p = 0.0031) was more enriched in minewells compared to seafloor sediments (Supplementary Figure 5). Most enriched ASVs (Figure 2D) exhibited modest $\log_2$ fold changes (<1), likely reflecting the environmental relevant contaminant concentrations observed in this study (TNT in the ng kg^{-1} range), which may limit the selective enrichment of tolerant taxa.

Taxonomic diversification within these families further distinguished minewell communities. Among 605 ASVs unique to minewells, 33 (5.45%) belonged to *Rhodobacteraceae*, compared to only 7 of 713 (0.98%) ASVs unique to seafloor sediments (Fisher's exact test, odds ratio = 5.82, p = 2.35 × 10^{-6}; Figure 2A). *Haliaceae* showed a similar pattern, with 31 of 605 (5.12%) minewell-unique ASVs versus 15 of 713 (2.10%) seafloor-unique ASVs (odds ratio = 2.51, p = 0.004; Figure 2A). This combination of increased relative abundance and significantly expanded ASV richness suggests that members of *Rhodobacteraceae* and *Haliaceae* may harbour metabolic traits conferring a proliferative advantage under minewell conditions, although the basis for this enrichment cannot be inferred from community composition data alone.

Several taxa within these families have established roles in contaminant degradation. Two upregulated ASVs belonged to *Rhodobacteraceae* genera *Sulfitobacter* and

Dinoroseobacter (Figure 2D). Genus *Sulfitobacter* degrades dimethylsulfoniopropionate[51] and petroleum-derived hydrocarbons[52], while the broader *Rhodobacteraceae* family shows elevated abundance at PAH-contaminated shipwreck sites[16] and harbors multiple hydrocarbon-degrading taxa in surface sediments[53,54]. *Halioglobus* (family *Haliaceae*) represents an emerging hydrocarbon-degrading taxon that may contribute to pollutant breakdown in minewells[55]. The prevalence of DNA repair genes and known contaminant-degrading capabilities, such as TNT metabolism, within Proteobacteria further supports their adaptive advantage in contaminated environments[15,56]. Together, these observations suggest that the enrichment of *Rhodobacteraceae* and *Haliaceae* in minewells may reflect ecological functions that promote persistence under contaminant stress.

Thirty-one ASVs showed reduced abundance in minewells compared to the seafloor, primarily from Acidobacteriota, Bacteroidota, and Myxococcota (Figure 2D). Within *Pirellulaceae*, six ASVs declined, including *Blastopirellula* and *Rhodopirellula*. *Flavobacteriaceae* showed five reduced ASVs, including *Aquibacter* and *Articiflavibacter*. *Algibacter* was an exception, with two ASVs displaying the highest $\log_2$ fold increases (1.61 and 1.83), potentially reflecting its ecological preference for complex algal polysaccharides that may accumulate in minewell microenvironments[57]. The imbalance between declining (31 ASVs) and increasing (11 ASVs) taxa suggests that minewell conditions may primarily filter out organisms sensitive to the contaminated environment, rather than enriching resistant ones. This interpretation is consistent with the subtly reduced alpha diversity (Figure 1A) and the increased prominence of Proteobacterial taxa, including the *Rhodobacteraceae* genera *Sulfitobacter* and *Dinoroseobacter*, as well

as *Halioglobus* (*Haliaceae*), which have previously been linked to contaminant degradation and persistence in polluted environments.

The resulting community shifts are compatible with an influence of contamination, such as TNT. The higher relative abundance and diversity of Proteobacteria in minewell sediments, particularly *Rhodobacteraceae* and *Halieaceae*, aligns with the metabolic versatility of these groups and their frequent occurrence in contaminant impacted environments[16,55]. At the broader class level, Alphaproteobacteria also showed enrichment in minewell sediments, consistent with reports of elevated Alphaproteobacterial representation in nitroaromatic-contaminated marine sediments and TNT-impacted soils[47,48,58]. Together, these observations support an association between contaminant exposure, such as TNT, and Proteobacterial restructuring.

2.4 Limited functional divergence across minewell and seafloor communities

To evaluate microbial functional potential across environments, metagenomic reads from minewell and seafloor samples were annotated and grouped into broad functional categories using Enzyme Commission (EC) numbers and Clusters of Orthologous Groups (COG) relative abundances (Figure 3A & Figure 3B). No statistically significant differences were detected between environments at this resolution, though functional potential appeared more conserved overall than taxonomic composition (Figure 1B). At finer resolution, multiple analyses revealed subtle but consistent functional shifts. Nonetheless, these analyses yielded moderate effect sizes and near-significant p-values for both broad COG functional categories ($R^2 = 0.57$, $p = 0.073$; Figure 3B) and EC

enzyme classes (R^2 = 0.52, p = 0.061; Figure 3A). At finer resolution, ordinations of EC specific classes and COG categories also overlapped between environments, yet PERMANOVA results again approached significance for EC (R^2 = 0.36, p = 0.059; Figure 3A) and COG classes (R^2 = 0.38, p = 0.061; Figure 3B).

The consistent convergence of p-values around 0.06 across analyses indicates that limited sample size, a constraint given the rarity and restricted accessibility of minewells, likely masks biologically meaningful functional trends. While functional differentiation is weaker than taxonomic divergence (Figure 1B), the repeated detection of moderate effect sizes supports the presence of functional restructuring between environments. The comparatively muted functional signal is consistent with functional redundancy, whereby taxonomically distinct communities retain overlapping metabolic capabilities, dampening detectable shifts in aggregate functional profiles despite underlying compositional change[59]. Importantly, conservation at broad functional resolution does not preclude adaptive specialization at finer scales. Environmental selection may act on a restricted subset of enzymes, leading to targeted shifts in specific EC and COG functions without dramatically altering global functional structure.

2.5 Functional enrichment in minewells aligns with contaminant-responsive enzyme classes

To characterize functional differences in microbial communities, gene function profiles were compared between minewell sediments and surrounding seafloor sediment samples based on metagenomic annotations. While overall functional profiles were broadly conserved between the two environments (Section 3.4) , targeted statistical

analysis identified specific functional categories that differed meaningfully. The relative abundance of EC and COG functional classes was therefore analysed across the two sample groups using DESeq2 with Benjamini–Hochberg correction (FDR < 0.1, $|\log_2 FC| > 0.6$; Figure 4A & Figure 4B). More functional classes were depleted than enriched in minewell communities relative to seafloor sediments (EC: 35 vs 26; COG: 27 vs 16), indicating broad functional contraction alongside targeted enrichment of specific metabolic capacities. Among enriched enzyme classes, oxidoreductases, involved in electron transfer and redox homeostasis were the most consistently overrepresented in minewell communities (Figure 4A). These included multiple $NAD(P)^+$-dependent dehydrogenases (EC 1.1.1.141, 1.1.1.357, 1.1.1.411, 1.1.1.420), amino-acid and nitrogen-related redox enzymes (EC 1.5.99.5, 1.7.3.3), thiol–disulfide oxidoreductases (EC 1.8.2.6), and diverse monooxygenase and dioxygenase families mediating O_2-dependent electron transfer (EC 1.13.11.41, 1.13.11.63, 1.13.11.78, 1.14.13.39, 1.14.13.238). Collectively, these enriched EC classes align with pathways involved in redox maintenance and detoxification (oxidoreductases), suggesting activation of metabolic functions commonly linked to cellular responses to chemical stress[60–62]. Consistent with this pattern, enriched COG categories included core components of the electron transport chain (COG2142, COG3761), redox-active enzymes involved in cofactor biosynthesis and reactive nitrogen signaling (COG2099, COG4362), and systems associated with detoxification and chemical stress tolerance (COG3853, COG4598)[63,64] (Figure 4B). Oxidoreductases as a broad functional category were significantly overrepresented in minewell communities. Oxidoreductases (EC) accounted for 57.7% of enriched enzyme classes in minewells, compared to 28.8% in seafloor

sediments (Fisher's exact test, odds ratio = 3.41, p = 0.035; Figure 4C), indicating a shift toward redox-driven metabolic strategies. The enrichment of oxidoreductases corresponds to metabolic activities linked to redox homeostasis and detoxification, processes frequently involved in microbial responses to environmental contamination[60,61].

To evaluate whether the functional shifts observed in minewell communities reflect responses to TNT exposure specifically, rather than generalised environmental difference, minewell metagenomic profiles were compared against a controlled laboratory TNT enrichment experiment in which sediment-derived microbial communities were exposed to high TNT concentrations of 80 mg L^{-1} (Section 2.3; Figure 4D & 4E). Figures 4D and 4E show the distribution of $\log_2$ fold changes from the enrichment experiment separately for enzyme classes and COG categories that were enriched versus depleted in minewell samples compared to the seafloor, allowing direct assessment of whether minewell-enriched functions respond consistently to experimental TNT stress. Enzyme classes enriched in minewell samples were significantly more likely to show positive $\log_2$ fold changes under TNT enrichment conditions than depleted classes (10/26 vs. 2/35; Fisher's exact test, odds ratio = 10.31, p = 0.0025; Figure 4D), with a consistent pattern observed for COG categories (11/16 vs. 7/27; odds ratio = 6.29, p = 0.0101; Figure 4E). Positive correlation occurred among functions associated with redox balancing and detoxification, including EC 1.8.2.6, EC 1.14.13.238, EC 1.5.99.5, and EC 1.1.1.411, as well as COG2142, COG3761, COG4598, and COG3853. These results indicate broadly concordant functional responses between environmental TNT exposure and experimental TNT stress, although the correspondence is not absolute, as expected of any comparison between in situ and laboratory systems. Minewell communities face complex contaminant

mixtures, variable redox conditions, and community-level interactions that cannot be fully reproduced in enrichment cultures[65–67], meaning some divergence in specific enriched functions is anticipated.

Nonetheless, these results show clear parallels between minewell microbiomes and the TNT enrichment, where TNT was the only selective pressure. This similarity indicates that contamination such as TNT in the minewells helps shape their functional profiles, particularly through higher levels of oxidoreductases and stress-response enzymes. These broad functions support tolerance to chemical stress, including exposure to TNT. Notably, nitroreductases and Old Yellow Enzymes, the enzyme classes most directly associated with TNT transformation, catalyzing the reduction of nitro groups and the aromatic ring, were not significantly enriched in the minewell microbiomes. This suggests that while the community adapts broadly to TNT-driven chemical stress, the capacity for direct TNT degradation is not a dominant selective outcome in the natural environment, in contrast to what might be expected from dedicated laboratory degradation studies.

2.6 Subtle enrichment of TNT-associated enzyme classes within the top 50 high-variance enzyme classes

To also capture enzyme classes exhibiting more subtle changes across samples, we ranked enzyme classes by the variance of DESeq2-normalized counts (Supplementary Figure 7 & Supplementary Figure 8). This approach also allows the identification of functions with moderate abundance differences, including those showing shifts between minewell and seafloor samples. Within this high-variance set, glutathione transferase (EC 2.5.1.18; COG0625) emerged as a possible TNT-associated marker. It was significantly

enriched in minewell sediments relative to seafloor samples (log_2 fold change = 0.29; *FDR* = 5 × 10^{-7}; Figure 5A) and showed a high proportional increase in the TNT enrichment experiment (80 mg L^{-1}), reaching 0.426% of assigned reads compared to 0.160% ± 0.008% in minewells and 0.130% ± 0.004% in seafloor sediments. The same trend appeared at the COG level, where glutathione transferase showed a similar log_2 fold change (0.30; *FDR* = 2 × 10^{-4}; Figure 5B) and increased relative abundance in the enrichment (0.398%) relative to seafloor (0.189 ± 0.013%) and minewell (0.234 ± 0.007%) samples.

Glutathione transferases (GSTs) are detoxification enzymes that conjugate glutathione to electrophilic or otherwise reactive compounds[68]. Because of this broad xenobiotic-processing role, GSTs are induced in organisms exposed to environmental contaminants[69]. Their involvement in TNT detoxification has been demonstrated in plants[70,71]. Bacterial GSTs have also been shown to respond to TNT exposure, although their specific roles in bacterial TNT-processing pathways remain poorly understood[15]. The high GST levels in the TNT enrichment, together with their increased abundance in minewell samples, suggest that GSTs may contribute to TNT detoxification in these microbial communities, through the formation of glutathione-conjugated intermediates[70,71]. GSTs were not classified among the enriched enzyme classes (Figure 4A & Figure 4B), as their log_2 fold change did not exceed the predefined threshold (log_2 fold > 0.6), despite a highly significant p-value. However, in the context of the measured environmental TNT concentrations, the modest but statistically robust increase observed here likely reflects a functional response at environmentally relevant exposure levels.

Several enzymes from the high-variance set, which showed higher abundances in minewell sediments, could also be relevant to TNT or nitroaromatic metabolism (Figure 5A & Figure 5B). These include aldehyde dehydrogenase (EC 1.2.1.3), aerobic carbon monoxide dehydrogenase (EC 1.2.5.3), glutamine synthetase (EC 6.3.1.2; *FDR* < 0.1), COG1012 dehydrogenase, and COG2124 cytochrome P450 (*FDR* < 0.1)[72–75]. Although only glutamine synthetase and COG 2124 cytochrome P450 reached statistical significance, the consistent directional shifts across these enzymes are notable given the TNT concentrations in situ (ng kg^{-1} range). As discussed earlier, microbial tolerance mechanisms may provide the physiological foundation that enables finer-scale TNT-transforming enzymes to function effectively, even when individual catabolic pathways show only low enrichment. When enzyme abundances are expressed as a percentage of assigned reads, these TNT-associated enzyme classes appear reduced in the enrichment experiment relative to environmental samples (Figure 5A & Figure 5B). The apparent reduction is likely a normalization artifact driven by the substantially higher annotation rate in the enrichment samples (~40%) compared with the environmental samples (~10%), which inflates the normalization denominator (Supplementary Figure 6). When abundances are normalized to total reads, the absolute abundance of TNT-associated enzymes in the enrichment experiment increases consistently (Supplementary Figure 9). In addition, these enzyme classes represent broad functional categories that participate in multiple metabolic processes, which may limit their apparent enrichment as other specialized functions expand in the enrichment conditions.

Well-characterized TNT degradation enzymes were analyzed separately and were part of the variance-based ranking. Nitroreductases (EC 1.7.1.16; COG0778) and Old Yellow

Enzymes/flavin oxidoreductases (EC 1.6.99.1; COG1902) showed no statistically significant differences between minewell and seafloor samples (Figure 5C & Figure 5D). However, mean abundances were consistently higher in minewells. In the TNT enrichment experiment, both enzyme classes increased at the EC level: EC 1.7.1.16 reached 0.0146% of total reads compared to 0.00806% ± 0.00024% in seafloor and 0.00875% ± 0.00126% in minewells, while EC 1.6.99.1 increased to 0.0550% compared to 0.0489% ± 0.00239% and 0.0542% ± 0.00083%, respectively. No corresponding increase was observed at the COG level, likely due to broader functional classification and assignment bias (Supplementary Figure 10).

TNT was reduced to intermediates, including 2-ADNT and 4-ADNT (Table 1). Both abiotic and biotic processes contribute to TNT attenuation in marine environments, with photolytic and chemical degradation occurring alongside microbial transformation[8,9,41]. Canonical TNT-degrading enzyme classes were not strongly enriched in minewell communities (Figure 5). Instead, these communities showed a higher representation of oxidoreductases and stress-response enzymes, including glutathione S-transferases (Figure 4 & Figure 5). Together, these results suggest that minewell communities are structured to better tolerate chemical stress, possibly creating an ecological context in which specialized tolerant taxa, even if not strongly enriched at the gene level, can actively and efficiently help contribute to TNT transformation.

2.7 Taxonomic and genomic parallels to TNT enrichment community indicate adaptation to TNT-contaminated environments

The enrichment experiment yielded nine metagenome-assembled genomes (MAGs) with >80% completeness and <10% contamination (Supplementary Table 2). *Rhodobacteraceae*, including *Sulfitobacter pontiacus*, were prominent in the TNT enrichment experiment, mirroring their elevated representation in environmental samples (Figure 2 & Figure 6A). The most abundant MAGs, *Neptuniibacter pectenicula* (28.0%) and *Alloalcanivorax xenomutans* (32.1%) (Figure 6A), together with other taxa such as *Thalassospira*, *Marinobacter*, and *Porticoccus*, are well known for hydrocarbon and aromatic compound degradation[76–80], indicating metabolic traits that could support TNT tolerance or transformation. This functional potential is consistent with the preliminary chemical measurements: TNT concentrations added (80 mg L^{-1}) declined to 59,960 ± 2,830 mg L^{-1} (n_{tech} = 2) during incubation, accompanied by the accumulation of intermediate metabolites (Supplementary Table 3). Abiotic transformation is unlikely as seen in other experiments using equal setups[81].

Environmental mapping of MAG reads showed that *Marinobacter alexandrii* (minewell: 0.0196% ± 0.0021%; seafloor: 0.0157% ± 0.0015%), *Roseovarius lutimaris* (minewell: 0.0040% ± 0.0012%; seafloor: 0.0021% ± 0.0007%), and *Sulfitobacter pontiacus* (minewell: 0.0040% ± 0.0018%; seafloor: 0.0023% ± 0.0006%) were more abundant in minewell sediments than in seafloor samples (Figure 6B). Although only *Marinobacter* reached statistical significance (Mann–Whitney, $p < 0.05$) and overall abundances remained low, these patterns are consistent with the subtle community shifts expected

under environmental level TNT contamination. The greater variability in minewell samples, likely reflecting more heterogeneous microenvironments, may further mask these small but ecologically meaningful effects. For MAGs that did not show differences in abundance, this may suggest that even the TNT concentrations near UC-30, among the highest reported in marine sediments, are insufficient to confer a strong selective advantage. Nevertheless, their high abundance in the enrichment experiment demonstrates clear potential for TNT biotransformation at elevated exposure levels, and, as discussed earlier, the chemically stressed minewell environment may still allow these tolerant taxa to contribute effectively to TNT transformation despite limited enrichment.

Gene annotation of MAGs using BlastKOALA revealed multiple xenobiotic degradation pathways, with a focus on nitrotoluene degradation (Figure 6C). *Neptuniibacter pectenicula* contained five genes linked to this pathway, including hydrogenase large and small subunits and N-ethylmaleimide reductase (nemA), part of the Old Yellow Enzyme family (COG1902, EC 1.6.99.1). The Old Yellow Enzyme family also showed a subtle, although not significant, increase in abundance in minewell samples compared to seafloor samples (Figure 5C & Figure 5D), suggesting it likely plays a central role in TNT transformation in marine environments. *Roseovarius lutimaris, Sulfitobacter pontiacus*, and *Salinisphaera* sp. also possessed nemA, supporting the probable contribution of *Rhodobacteraceae* to TNT biotransformation. *Neptuniibacter pectenicula* also carried multiple genes for toluene and xylene degradation. Because toluene is proposed as a TNT intermediate[82], the presence of a complete toluene and xylene degradation pathway (Supplementary Figure 11) suggests that marine microbes, particularly *Neptuniibacter*, may have the metabolic potential to fully mineralize TNT. This is consistent with the

chemical data from the enrichment, where TNT concentrations decreased (Supplementary Table 3).

The absence of *Haliaceae* in the laboratory enrichment may reflect sensitivity to elevated TNT concentrations, substrate specificity, or requirements for environmental conditions not replicated in the lab, such as pressure, salinity, microbial interactions, or trace elements. Alternatively, *Haliaceae* may preferentially degrade hydrocarbons associated with the shipwreck rather than TNT, as fuel residues (e.g. diesel, bunker fuel) and structural materials such as paints and coatings are well-documented sources of hydrocarbon contamination in shipwreck environments and represent likely substrates for such taxa[16,55,83]. Stochastic factors, including random extinction during sample handling, may also contribute. Targeted studies on TNT tolerance and hydrocarbon dependency are needed to clarify the ecological niche of *Haliaceae* in contaminated sediments.

In the minewell samples, members of the *Rhodobacteraceae* were consistently enriched (Figure 2A & Figure 2B), mirroring their presence in the TNT enrichment cultures (Figure 6A). All recovered MAGs belonged to Proteobacteria, supporting a close taxonomic overlap between the in situ microbial community and the taxa that responded under controlled TNT exposure (Figure 2B & Figure 2D). Several of these Proteobacteria MAGs encoded genes associated with the nitrotoluene degradation pathway, including the Old Yellow Enzyme NemA (Figure 6C). Together with the observed decrease in TNT concentration, this may indicates that these functional traits are expressed under TNT exposure. Given the parallels with the minewell environment, it is therefore more likely that similar TNT-transforming capabilities are present within the minewell communities.

3. Conclusion

This study provides one of the first detailed characterizations of a marine sediment microbiome chronically exposed to leaking munitions and reveals how long-term contamination can shape both community structure and functional potential. Minewell sediments, located within the TNT-impacted interior of a corroding wreck, displayed distinct taxonomic shifts, including enrichment of Proteobacteria such as *Haliaceae* and *Rhodobacteraceae*. Functional profiling further showed elevated levels of oxidoreductases and stress-response enzyme classes, consistent with microbial adaptation to enriched TNT exposure.

The overall community structure and functional profiles of minewell sediments showed stronger parallels with the TNT-only enrichment experiment than with the adjacent seafloor. While many taxa occur across both environments, the minewell communities exhibited compositional and functional shifts that mirror those observed under controlled TNT exposure. This suggests that chronic contamination creates ecological conditions that favor stress-tolerant lineages and functions, resulting in communities that are better adapted to withstand and potentially transform TNT. The enrichment experiment, which demonstrated active TNT removal, reinforces this interpretation by revealing similar functional signatures under defined exposure conditions.

These results indicate that contaminated minewell environments exert selective pressures that shape microbial assemblages toward enhanced stress tolerance and potential transformation capacity. While this study specifically focused on TNT, the observed patterns likely reflect broader microbial responses to chronic contaminant

exposure rather than TNT alone. Co-occurring contaminants and environmental factors also contribute to community structuring, and similar adaptive trajectories are therefore expected under exposure to other pollutants. By demonstrating this effect for TNT, our findings provide a framework that can be extended to investigate microbial adaptation, metabolic versatility, and natural attenuation processes across a wider range of contaminated marine sediments.

4. Materials and Methods

4.1 Wreck selection and sampling

The SM UC-30, a German Type UC II minelaying submarine sunk on 21 April 1917 during World War I, was selected due to its high contamination potential. The wreck lies at ~55°31'N, 7°57'E at 23 m depth in a major tidal inlet of the Wadden Sea. The wreck was discovered in 2016 by the Danish company JD-Contractor. Subsequent diving inspections and multibeam sonar survey by the Royal Danish Navy and Aarhus University, confirmed the presence of 18 UC 200 mines (200 kg TNT each) and six G/6 torpedoes (160 kg Hexanite; 60% TNT), with additional 8.8 cm ammunition likely remaining[20]. Visual surveys showed several corroded, partially exposed mines with TNT in direct contact with seawater (Supplementary Figure 2).

To characterize contaminant distribution, 23 sediment samples were collected by Danish Navy divers on 23 September 2020 (Figure 7). Five proximal samples were taken from within the minewells (0–5 cm depth) to assess primary TNT release, seven distal samples were collected within 1 m of the hull to evaluate lateral spread, and one reference sample

taken 10 m away. Sediments were retrieved using 0.5 L plastic bottles scraped across the uppermost centimeter. Onboard, samples were drained, weighed (40–180 g), and split into two subsamples for analyses in Gent, Belgium (Ghent University), and Kiel, Germany (Kiel University). All material was stored on dry ice, kept frozen at Aarhus University, and shipped on 28 September 2020 in insulated containers. Due to the highly restricted nature of the site, sampling was necessarily limited (Supplementary Figure 2).

4.2 TNT compound analysis

Sediment samples were prepared as described previously[21]. To establish baseline results, 2 g of freeze-dried sediment was extracted with acetonitrile, concentrated to 0.6 mL using a rotary vacuum concentrator, transferred to 1.5 mL brown glass vials, and analyzed by GC-MS/MS. Samples were then reprocessed using 100 g of material. For this, 100 g of wet sediment was mixed with 250 mL of ultrapure water, spiked with 25 ng of $^{13}C^{15}N$-TNT as internal standard, shaken for 80 minutes, and sonicated for 15 minutes. The samples were subsequently centrifuged at 4,500 rpm (10 °C) for 15 minutes, filtered through a 595 1/2 pleated filter, and applied to SPE columns under mild vacuum. The columns were dried for 30 minutes under vacuum, eluted with 4 mL of acetonitrile, concentrated to 600 µL, and stored at -20 °C in 1.5 mL amber vials.

All samples were measured in duplicates on a Thermo Fisher Scientific Trace 1310 gas chromatograph coupled to a TSQ 8000 Evo triple quadrupole mass spectrometer (GC-MS/MS)[28]. Separation was performed on a TraceGold TG-5MS amine column (15 m × 0.25 mm × 0.25 µm; Thermo Fisher Scientific Inc., Waltham, MA, USA). One microliter of each sample was injected in splitless mode using quartz wool liners. Quantification was

carried out using external calibration curves. Spectra were recorded and analyzed using Chromeleon 7.2 (Thermo Fisher Scientific Inc., Waltham, MA, USA). Detection limits for the 2 g and 100 g methods were as follows: TNT: 0.050 / 0.006 µg/kg; 4-ADNT: 0.030 / 0.003 µg/kg; 2-ADNT: 0.030 / 0.005 µg/kg; 2,4; DNT: 0.020 / 0.002 µg/kg; 1,3-DNB: 0.100 / 0.010 µg/kg

4.3 Laboratory incubation experiment

Sediment samples from the UC-30 wreck site were pooled (UC30 M2, UC30 M3, and UC30 Sf1) to obtain a representative inoculum. A TNT stock solution (TNT in 100% methanol; Royal Military Academy, Belgium) was added to sterile amber Duran bottles, yielding an initial TNT concentration of ~80 mg L^{-1}. Amber bottles were used to prevent photodegradation, and the concentration was chosen to remain below the TNT solubility limit (130 mg L^{-1} at 20 °C). The solvent was evaporated before adding nutrient-amended, filter-sterilized (0.22 µm) seawater to dissolve the TNT (Supplementary table S1). The resulting solution was inoculated with pooled sediment slurry (10% v/v) and incubated at ~20 °C with aeration (0.22 µm ePTFE membrane filters) for 12 weeks to allow adaptation and proliferation of TNT responsive microorganisms. TNT and its transformation products were quantified at the end of the incubation to assess degradation dynamics.

4.4 16s RNA gene and Metagenomic shotgun sequencing

Genomic DNA was extracted from marine sediment samples using the DNeasy PowerSoil Pro Kit (Qiagen, Germany). PCR amplification was performed with recombinant Taq DNA Polymerase (Thermo Fisher Scientific, Waltham, USA) in 25 µL reaction volumes containing: 2.5 µL of 10× Taq buffer (+KCl, –$MgCl_2$), 0.5 µL of 10 mM

dNTPs, 1.5 µL of 25 mM $MgCl_2$, 0.5 µL each of 10 µM primers 27f (AGAGTTTGATCMTGGCTCAG) and 1492r (TACGGYTACCTTGTTACGACTT), 0.125 µL of 5 U/µL Taq polymerase, 0.065 µL of 20 mg/mL BSA (Roche, Basel, Switzerland), 14.81 µL of PCR-grade water, and 1 µL of DNA template. Two samples were processed in triplicate to assess reproducibility, and negative controls for extraction and PCR confirmed the absence of contamination. Thermal cycling consisted of 95 °C for 7 min; 30 cycles of 95 °C for 1 min, 55 °C for 1 min, and 72 °C for 2 min; followed by 72 °C for 10 min. PCR products and DNA extracts were checked on 2% agarose gels to verify amplification and fragment size. A total of 10 µL of each genomic DNA extract was submitted to LGC Genomics (Berlin, Germany) for library preparation and Illumina MiSeq sequencing (v3 chemistry, 2×300 bp paired-end) using primers 341F (5'-CCT ACG GGN GGC WGC AG-3') and 785Rmod (5'-GAC TAC HVG GGT ATC TAA KCC-3'), targeting the V3–V4 hypervariable regions of the 16S rRNA gene.

Metagenomic libraries, pools of adapter-tagged DNA fragments derived from total community DNA, were prepared using the Nextera XT DNA Library Preparation Kit (Illumina, San Diego, USA) according to the manufacturer's protocol. Paired-end sequencing (2 × 150 bp) was performed on an Illumina HiSeq 2500.

4.5 Bioinformatic analysis of amplicon and metagenomic data

All amplicon data were processed in R (v4.0.3) using DADA2 following the standard workflow[22]. Primer sequences were removed, reads were quality-filtered (truncQ = 2; maxEE = 2,2), and sequences containing ambiguous bases were discarded. After dereplication, denoising was performed using the DADA error model with pooled sample

inference, and paired reads were merged. Chimera-free amplicon sequence variants (ASVs) were assigned taxonomy using the SILVA v138 database[23]. ASVs classified as Archaea, mitochondria, and chloroplasts, as well as singleton taxonomic assignments, were removed.

Metagenome-assembled genomes (MAGs) were reconstructed using the MetaWRAP (v1.3.2) pipeline[24]. Within this framework, quality-filtered reads were assembled into contigs with MEGAHIT[25] and binned independently using MaxBin2[26], MetaBAT2[27], and CONCOCT[28]. The resulting bin sets were automatically consolidated and refined using MetaWRAP's bin-refinement module, retaining bins with ≥80% completeness and ≤10% contamination. This process yielded nine MAGs. Genome quality was assessed using CheckM[29], and relative MAG abundances were estimated using MetaWRAP's abundance estimation module. Taxonomic assignments were generated with GTDB-Tk (v2.4.1)[30]. Quality-controlled reads were mapped to contigs with Bowtie2(v2.5.4)[31] and processed with SAMtools (v1.3)[32]. Functional profiling used the DIAMOND+MEGAN6[33] workflow: reads were aligned to the NCBI-nr[34] database in *blastx* mode and the resulting alignment files were imported into MEGAN for taxonomic and functional assignment. ORFs were predicted with Prodigal[35], and annotated using BlastKOALA[36].

4.6 Statistical data analysis

Data analysis was conducted in R using Phyloseq (v1.22.3)[37] for ASV processing, vegan (v2.5.6)[38], and iNEXT[39] for diversity estimation. Differential abundance of ASVs and enzyme classes was assessed with DESeq2 (v2)[40], using a Benjamini–Hochberg FDR threshold of 0.1 and a $\log_2$ fold change cutoff of 0.6 to account for limited sample size and

subtle effect sizes. To ensure robustness, ASVs were filtered to retain only those present in ≥60% of samples and exceeding a minimum prevalence threshold (1.6). Group differences were evaluated using Mann–Whitney U ($p = 0.05$) and Fisher's exact tests ($\alpha = 0.05$). Community composition data were Hellinger transformed, ordinated using Bray–Curtis NMDS, and compared among sampling locations using PERMANOVA (adonis2, 999 permutations), with dispersion homogeneity assessed via betadisper.

5. Acknowledgements

We thank Uwe Wichert for the historical information about the UC-30 submarine and the munitions aboard. The Royal Danish Navy divers are thanked for professional service and help with the sediment sampling. We further thank EIVA for providing academic software licenses for SeisLab Aarhus, Aarhus University used for the processing of the multibeam echosounder data. The authors also thank the editor and the anonymous reviewers for their time and valuable feedback during the review process.

6. Author contributions

Rune Vuerstaek – Writing, Data analysis, visualization – Original draft
Jasmine Heyse – Investigation
Tim Lacoere – Software, visualization, investigation
Lillian Tabea Hannah Buenning – Methodology, investigation
Maarten De Rijcke – Writing-Review and editing
Edmund Maser – Methodology, investigation, Writing-Review and editing
Katrine Juul Andresen – Visualization, Data acquisition, Writing-Review and editing
Nico Boon – Conceptualization, Writing-Review and editing, Funding acquisition
Kankana Kundu – Conceptualization, Editing and reviewing, Project administration, Funding acquisition, Supervision

7. Data availability

Raw sequencing data (16S rRNA amplicon and shotgun metagenomic) generated in this study have been deposited in the NCBI Sequence Read Archive under BioProject accession PRJNA1478556.

8. Code Availability

No custom code was generated in this study. All bioinformatic analyses were performed using publicly available software and packages as described in the Materials and Methods.

9. Funding

The research leading to the results presented in this publication was carried out with infrastructure funded by the FWO-SBO grant ("DisARM", grant no. 616861) and by the BOF24/DOC/014 Blue Growth label. The Interreg North Sea Region program funded the North Sea Wrecks (NSW) project during which the sampling and multibeam scanning of UC-30 were performed.

10. Conflict of interest

The authors declare that the research was conducted in the absence of any commercial or financial relationships that could be construed as a potential conflict of interest.

11. Supplementary material

The Supplementary Material for this article can be found attached

12. References

1. Sunagawa, S. *et al.* Structure and function of the global ocean microbiome. *Science* **348**, 1261359 (2015).
2. Logares, R. Decoding populations in the ocean microbiome. *Microbiome* **12**, 67 (2024).
3. Chen, J. *et al.* Global marine microbial diversity and its potential in bioprospecting. *Nature* **633**, 371–379 (2024).
4. Tornero, V. & Hanke, G. Chemical contaminants entering the marine environment from sea-based sources: A review with a focus on European seas. *Mar. Pollut. Bull.* **112**, 17–38 (2016).
5. Koide, S., Silva, J. A. K., Dupra, V. & Edwards, M. Bioaccumulation of chemical warfare agents, energetic materials, and metals in deep-sea shrimp from discarded military munitions sites off Pearl Harbor. *Deep Sea Res. Part II Top. Stud. Oceanogr.* **128**, 53–62 (2016).
6. Beck, A. J. *et al.* Spread, Behavior, and Ecosystem Consequences of Conventional Munitions Compounds in Coastal Marine Waters. *Front. Mar. Sci.* **5**, (2018).
7. Böttcher, K., Rühl, S. & Wichert, W. Munitionsbelastung der deutschen Meeresgewässer - Bestandsaufnahme und Empfehlungen.
8. Chappell, M. A., Porter, B. E., Price, C. L., Pettway, B. A. & George, R. D. Differential kinetics and temperature dependence of abiotic and biotic processes controlling the environmental fate of TNT in simulated marine systems. *Mar. Pollut. Bull.* **62**, 1736–1743 (2011).

9. Luning Prak, D. J., Breuer, J. E. T., Rios, E. A., Jedlicka, E. E. & O'Sullivan, D. W. Photolysis of 2,4,6-trinitrotoluene in seawater and estuary water: Impact of pH, temperature, salinity, and dissolved organic matter. *Mar. Pollut. Bull.* **114**, 977–986 (2017).
10. Strehse, J. S., Brenner, M., Kisiela, M. & Maser, E. The explosive trinitrotoluene (TNT) induces gene expression of carbonyl reductase in the blue mussel (Mytilus spp.): a new promising biomarker for sea dumped war relicts? *Arch. Toxicol.* **94**, 4043–4054 (2020).
11. Juhasz, A. L. & Naidu, R. Explosives: Fate, Dynamics, and Ecological Impact in Terrestrial and Marine Environments. in *Reviews of Environmental Contamination and Toxicology* 163–215 (Springer, New York, NY, 2007). doi:10.1007/978-0-387-69163-3_6.
12. Schuster, R. M. *et al.* Environmental risks from world war shipwrecks: Field-based biomarker evidence from caged mussels in the North Sea. *Mar. Pollut. Bull.* **229**, 119738 (2026).
13. Smets, B. F., Yin, H. & Esteve-Nuñez, A. TNT biotransformation: when chemistry confronts mineralization. *Appl. Microbiol. Biotechnol.* **76**, 267–277 (2007).
14. Yin, M. *et al.* Oxygen-insensitive nitroreductase bacteria-mediated degradation of TNT and proteomic analysis. *Environ. Sci. Pollut. Res.* **30**, 116227–116238 (2023).
15. Cabrera, Ma. Á., Márquez, S. L. & Pérez-Donoso, J. M. New insights into xenobiotic tolerance of Antarctic bacteria: transcriptomic analysis of Pseudomonas sp. TNT3 during 2,4,6-trinitrotoluene biotransformation. *Environ. Sci. Pollut. Res.* **31**, 17256–17274 (2024).
16. Van Landuyt, J. *et al.* 80 years later: Marine sediments still influenced by an old war ship. *Front. Mar. Sci.* **9**, (2022).
17. Beck, A. J. *et al.* Widespread environmental contamination from relic munitions in the southwestern Baltic Sea. *Chemosphere* **372**, 144115 (2025).

18. den Otter, J. H. *et al.* Release of Ammunition-Related Compounds from a Dutch Marine Dump Site. *Toxics* **11**, 238 (2023).

19. Beck, A. J. *et al.* Spread, Behavior, and Ecosystem Consequences of Conventional Munitions Compounds in Coastal Marine Waters. *Front. Mar. Sci.* **5**, (2018).

20. Andresen, K. J. Redaktion: Katrine Juul Andresen.

21. Bünning, T. H., Strehse, J. S., Hollmann, A. C., Bötticher, T. & Maser, E. A Toolbox for the Determination of Nitroaromatic Explosives in Marine Water, Sediment, and Biota Samples on Femtogram Levels by GC-MS/MS. *Toxics* **9**, 60 (2021).

22. Callahan, B. J. *et al.* DADA2: High resolution sample inference from Illumina amplicon data. *Nat. Methods* **13**, 581–583 (2016).

23. Quast, C. *et al.* The SILVA ribosomal RNA gene database project: improved data processing and web-based tools. *Nucleic Acids Res.* **41**, D590–D596 (2013).

24. Uritskiy, G. V., DiRuggiero, J. & Taylor, J. MetaWRAP—a flexible pipeline for genome-resolved metagenomic data analysis. *Microbiome* **6**, 158 (2018).

25. Li, D., Liu, C.-M., Luo, R., Sadakane, K. & Lam, T.-W. MEGAHIT: an ultra-fast single-node solution for large and complex metagenomics assembly via succinct de Bruijn graph. *Bioinformatics* **31**, 1674–1676 (2015).

26. Wu, Y.-W., Simmons, B. A. & Singer, S. W. MaxBin 2.0: an automated binning algorithm to recover genomes from multiple metagenomic datasets. *Bioinformatics* **32**, 605–607 (2016).

27. Kang, D. D. *et al.* MetaBAT 2: an adaptive binning algorithm for robust and efficient genome reconstruction from metagenome assemblies. *PeerJ* **7**, e7359 (2019).

28. Alneberg, J. *et al.* Binning metagenomic contigs by coverage and composition. *Nat. Methods* **11**, 1144–1146 (2014).

29. Parks, D. H., Imelfort, M., Skennerton, C. T., Hugenholtz, P. & Tyson, G. W. CheckM: assessing the quality of microbial genomes recovered from isolates, single cells, and metagenomes. *Genome Res.* **25**, 1043–1055 (2015).

30. Chaumeil, P.-A., Mussig, A. J., Hugenholtz, P. & Parks, D. H. GTDB-Tk v2: memory friendly classification with the genome taxonomy database. *Bioinformatics* **38**, 5315–5316 (2022).

31. Langmead, B. & Salzberg, S. L. Fast gapped-read alignment with Bowtie 2. *Nat. Methods* **9**, 357–359 (2012).

32. Danecek, P. *et al.* Twelve years of SAMtools and BCFtools. *GigaScience* **10**, giab008 (2021).

33. Bağcı, C., Patz, S. & Huson, D. H. DIAMOND+MEGAN: Fast and Easy Taxonomic and Functional Analysis of Short and Long Microbiome Sequences. *Curr. Protoc.* **1**, e59 (2021).

34. Sayers, E. W. *et al.* Database resources of the National Center for Biotechnology Information in 2025. *Nucleic Acids Res.* **53**, D20–D29 (2025).

35. Hyatt, D. *et al.* Prodigal: prokaryotic gene recognition and translation initiation site identification. *BMC Bioinformatics* **11**, 119 (2010).

36. Kanehisa, M., Sato, Y. & Morishima, K. BlastKOALA and GhostKOALA: KEGG Tools for Functional Characterization of Genome and Metagenome Sequences. *J. Mol. Biol.* **428**, 726–731 (2016).

37. McMurdie, P. J. & Holmes, S. phyloseq: An R Package for Reproducible Interactive Analysis and Graphics of Microbiome Census Data. *PLOS ONE* **8**, e61217 (2013).

38. Dixon, P. VEGAN, a package of R functions for community ecology. *J. Veg. Sci.* **14**, 927–930 (2003).

39. Hsieh, T. C., Ma, K. H. & Chao, A. iNEXT: an R package for rarefaction and extrapolation of species diversity (Hill numbers). *Methods Ecol. Evol.* **7**, 1451–1456 (2016).

40. Love, M. I., Huber, W. & Anders, S. Moderated estimation of fold change and dispersion for RNA-seq data with DESeq2. *Genome Biol.* **15**, 550 (2014).

41. Walker, S. W. *et al.* Mineralization of 2,4,6-Trinitrotoleune (TNT) in Coastal Waters and Sediments. https://apps.dtic.mil/sti/html/tr/ADA456842/ (2006).

42. Boparai, H. K. *et al.* Abiotic transformation of high explosives by freshly precipitated iron minerals in aqueous FeII solutions. *Chemosphere* **79**, 865–872 (2010).

43. Ariyarathna, T. *et al.* Biodegradation and mineralization of isotopically labeled TNT and RDX in anaerobic marine sediments. *Environ. Toxicol. Chem.* **36**, 1170–1180 (2017).

44. Claus, H. *et al.* Transformation of 2,4,6-trinitrotoluene (TNT) by Raoultella terrigena. *Biodegradation* **18**, 27–35 (2007).

45. Gumuscu, B. & Tekinay, T. Effective biodegradation of 2,4,6-trinitrotoluene using a novel bacterial strain isolated from TNT-contaminated soil. *Int. Biodeterior. Biodegrad.* **85**, 35–41 (2013).

46. Delaunay, E., Jouanneau, S., Durand, M.-J. & Thouand, G. Evaluating toxic impact on marine microbial community using combined genetic and phenotypic approaches. *Environ. Sci. Pollut. Res.* **31**, 66120–66135 (2024).

47. Zhang, H. *et al.* Spatial-vertical variations of energetic compounds and microbial community response in soils from an ammunition demolition site in China. *Sci. Total Environ.* **875**, 162553 (2023).

48. Yang, X. *et al.* Microbial community structure and metabolome profiling characteristics of soil contaminated by TNT, RDX, and HMX. *Environ. Pollut.* **285**, 117478 (2021).

49. Luo, J. *et al.* Variations of microbiota in three types of typical military contaminated sites: Diversities, structures, influence factors, and co-occurrence patterns. *J. Hazard. Mater.* **443**, 130290 (2023).

50. Travis, E. R., Bruce, N. C. & Rosser, S. J. Microbial and plant ecology of a long-term TNT-contaminated site. *Environ. Pollut.* **153**, 119–126 (2008).

51. He, Z. *et al.* Complete genome sequence of *Sulfitobacter pontiacus* WPMT18310, a dimethylsulfoniopropionate (DMSP) degradation bacterium isolated from the Mariana Trench. *Mar. Genomics* **79**, 101151 (2025).

52. Mugge, R. L., Lee, J. S., Brown, T. T. & Hamdan, L. J. Marine biofilm bacterial community response and carbon steel loss following Deepwater Horizon spill contaminant exposure. *Biofouling* **35**, 870–882 (2019).

53. Buchan, A., González, J. M. & Chua, M. J. Aerobic Hydrocarbon-Degrading Alphaproteobacteria: Rhodobacteraceae (Roseobacter). in *Taxonomy, Genomics and Ecophysiology of Hydrocarbon-Degrading Microbes* (ed. McGenity, T. J.) 1–13 (Springer International Publishing, Cham, 2019). doi:10.1007/978-3-319-60053-6_8-1.

54. Lin, W. *et al.* Microbial community assembly responses to polycyclic aromatic hydrocarbon contamination across water and sediment habitats in the Pearl River Estuary. *J. Hazard. Mater.* **457**, 131762 (2023).

55. Chen, S.-C., Musat, F., Richnow, H.-H. & Krüger, M. Microbial diversity and oil biodegradation potential of northern Barents Sea sediments. *J. Environ. Sci.* **146**, 283–297 (2024).

56. Boopathy, R., Wilson, M., Montemagno, C. D., Manning, J. F. & Kulpa, C. F. Biological transformation of 2,4,6-trinitrotoluene (TNT) by soil bacteria isolated from TNT-contaminated soil. *Bioresour. Technol.* **47**, 19–24 (1994).

57. Liu, A., Wang, H., Yang, Y.-Y., Xue, Q.-J. & Li, X.-Z. Reclassification of Algibacter wandonensis as a Later Heterotypic Synonym of Algibacter lectus Based on Whole-Genome Sequence Analysis. *Curr. Microbiol.* **78**, 1034–1038 (2021).

58. Yang, H., Zhao, J. -S. & Hawari, J. Effect of 2,4-dinitrotoluene on the anaerobic bacterial community in marine sediment. *J. Appl. Microbiol.* **107**, 1799–1808 (2009).

59. Louca, S. *et al.* Function and functional redundancy in microbial systems. *Nat. Ecol. Evol.* **2**, 936–943 (2018).

60. Cárdenas-Moreno, Y., González-Bacerio, J., García Arellano, H. & del Monte-Martínez, A. Oxidoreductase enzymes: Characteristics, applications, and challenges as a biocatalyst. *Biotechnol. Appl. Biochem.* **70**, 2108–2135 (2023).

61. Bilal, M. *et al.* Oxidoreductases as a versatile biocatalytic tool to tackle pollutants for clean environment – a review. *J. Chem. Technol. Biotechnol.* **97**, 420–435 (2022).

62. Wang, Y., Li, J. & Liu, A. Oxygen activation by mononuclear nonheme iron dioxygenases involved in the degradation of aromatics. *J. Biol. Inorg. Chem. JBIC Publ. Soc. Biol. Inorg. Chem.* **22**, 395–405 (2017).

63. Carrera-Reyna, M., Cruz-Flores, E. & Merino, E. Analysis and comparison of the bacterial σ54 regulon: Evidence of phylogenetic trends in gene regulation. *PLOS One* **20**, e0327805 (2025).

64. Nguyen, T. T. H., Kikuchi, T., Tokunaga, T., Iyoda, S. & Iguchi, A. Diversity of the Tellurite Resistance Gene Operon in Escherichia coli. *Front. Microbiol.* **12**, (2021).

65. Langenheder, S. & Lindström, E. S. Factors influencing aquatic and terrestrial bacterial community assembly. *Environ. Microbiol. Rep.* **11**, 306–315 (2019).

66. Goutam Mukherjee, A. *et al.* Mixed Contaminants: Occurrence, Interactions, Toxicity, Detection, and Remediation. *Mol. Basel Switz.* **27**, 2577 (2022).

67. Borch, T. *et al.* Biogeochemical Redox Processes and their Impact on Contaminant Dynamics. *Environ. Sci. Technol.* **44**, 15–23 (2010).

68. Allocati, N., Federici, L., Masulli, M. & Di Ilio, C. Glutathione transferases in bacteria. *FEBS J.* **276**, 58–75 (2009).

69. Lloyd-Jones, G. & Lau, P. C. Glutathione S-transferase-encoding gene as a potential probe for environmental bacterial isolates capable of degrading polycyclic aromatic hydrocarbons. *Appl. Environ. Microbiol.* **63**, 3286–3290 (1997).

70. Tzafestas, K. *et al.* Expression of a Drosophila glutathione transferase in Arabidopsis confers the ability to detoxify the environmental pollutant, and explosive, 2,4,6-trinitrotoluene. *New Phytol.* **214**, 294–303 (2017).

71. Gunning, V. *et al.* Arabidopsis Glutathione Transferases U24 and U25 Exhibit a Range of Detoxification Activities with the Environmental Pollutant and Explosive, 2,4,6-Trinitrotoluene. *Plant Physiol.* **165**, 854–865 (2014).

72. Cabrera, Ma. Á., Márquez, S. L. & Pérez-Donoso, J. M. New insights into xenobiotic tolerance of Antarctic bacteria: transcriptomic analysis of Pseudomonas sp. TNT3 during 2,4,6-trinitrotoluene biotransformation. *Environ. Sci. Pollut. Res.* **31**, 17256–17274 (2024).

73. Xu, M. *et al.* Degradation of 2,4,6-Trinitrotoluene (TNT): Involvement of Protocatechuate 3,4-Dioxygenase (P34O) in Buttiauxella sp. S19-1. *Toxics* **9**, 231 (2021).

74. Yang, X., Yin, M., Zhu, Y., Zhao, S. & Xi, H. Key genomes, transcriptomes, proteins, and metabolic factors involved in the detoxification/tolerance of TNT and its intermediates by bacteria in anaerobic/aerobic environments. *J. Hazard. Mater.* **478**, 135489 (2024).

75. Yang, X., Zhu, Y., Zhao, S. & Xi, H. Reconstruction of a microbial TNT deep degradation system and its mechanism for reshaping microecology. *J. Hazard. Mater.* **488**, 137411 (2025).

76. Achberger, A. M. *et al.* Bacteria-Oil Microaggregates Are an Important Mechanism for Hydrocarbon Degradation in the Marine Water Column. *mSystems* **6**, 10.1128/msystems.01105-21 (2021).

77. Santisi, S. *et al.* Biodegradation Potential of Oil-degrading Bacteria Related to the Genus Thalassospira Isolated from Polluted Coastal Area in Mediterranean Sea. *Soil Sediment Contam. Int. J.* **31**, 316–332 (2022).

78. Xu, X. *et al.* Petroleum Hydrocarbon-Degrading Bacteria for the Remediation of Oil Pollution Under Aerobic Conditions: A Perspective Analysis. *Front. Microbiol.* **9**, (2018).

79. Davila-Santiago, L. *et al.* Microbial diversity in a military impacted lagoon (Vieques, Puerto Rico) and description of "*Candidatus* Biekeibacterium resiliens" gen. nov., sp. nov. comprising a new bacterial family. *Syst. Appl. Microbiol.* **45**, 126288 (2022).

80. Gutierrez, T., Nichols, P. D., Whitman, W. B. & Aitken, M. D. Porticoccus hydrocarbonoclasticus sp. nov., an Aromatic Hydrocarbon-Degrading Bacterium Identified in Laboratory Cultures of Marine Phytoplankton. *Appl. Environ. Microbiol.* **78**, 628–637 (2012).

81. Kundu, K. *et al.* Enhanced removal of warfare agent tri-nitro-toluene by a *Methylophaga*-dominated microbiome. *Mar. Pollut. Bull.* **190**, 114866 (2023).

82. Esteve-Núñez, A., Caballero, A. & Ramos, J. L. Biological Degradation of 2,4,6-Trinitrotoluene. *Microbiol. Mol. Biol. Rev.* **65**, 335–352 (2001).

83. Thomas, G. E. *et al.* Evaluation of Polycyclic Aromatic Hydrocarbon Pollution From the HMS Royal Oak Shipwreck and Effects on Sediment Microbial Community Structure. *Front. Mar. Sci.* **8**, (2021).

Figure 1:

Caption: Microbial taxonomic community structure differs between minewells and the seafloor

Legend: Taxonomic alpha and beta diversity of Minewell and Seafloor microbial communities. ***(A)*** *Alpha diversity estimated using Hill numbers (q = 0, richness; q = 1, Shannon diversity; q = 2, Simpson diversity) shows no significant differences between Minewell and Seafloor samples.* ***(B)*** *Non-metric multidimensional scaling (NMDS) ordination based on Bray–Curtis dissimilarity of bacterial taxonomic composition reveals distinct clustering by location. Black lines connect technical replicates.*

Figure 2

Caption: Minewell-associated bacterial taxa are enriched in Proteobacteria, including Rhodobacteraceae and Halieaceae:

Legend: Taxonomic overlap and differential abundance of bacterial communities in Minewell and Seafloor samples. ***(A)*** *Lollipop chart showing the number of ASVs unique to minewell samples and unique to seafloor samples, grouped at the family level. Minewell samples had higher numbers of unique ASVs assigned to Rhodobacteraceae and Halieaceae compared to seafloor samples* ***(B)*** *Barplot of relative abundance (%) of Proteobacteria, showing higher proportions in Minewell samples than Seafloor. Families enriched in Minewells include Rhodobacteraceae and Halieaceae, highlighted in bold.* ***(C)*** *Venn diagram showing the number of unique and shared ASVs between Minewell and Seafloor samples.* ***(D)*** *Differential abundance analysis of bacterial ASVs between Minewell and Seafloor samples performed using DESeq2 (Benjamini–Hochberg correction, FDR < 0.1, $|log_2FC| > 0.5$) . Most ASVs enriched in Minewell samples (6 of 11) belonged to the phylum Proteobacteria, including members of the Rhodobacteraceae and Halieaceae*

Figure 3:

Caption: Functional gene profiles are broadly conserved between minewell and seafloor microbial communities

Legend: Functional profiles were largely conserved between minewell and seafloor microbial communities, with only subtle differences detected across environments. (Left) ***(A)*** *Cleveland-style dot plot of relative abundances (% Assigned Reads) of broad EC enzyme classes (EC1–EC7) in Minewell and seafloor samples.* ***(B)*** *Cleveland-style dot plot of relative abundances (% Assigned Reads) of broad COG functional categories (Metabolism, cellular processes and signaling, information storage and processing). (Right)* ***(A)*** *NMDS ordination based on Bray-Curtis dissimilarity of fine-resolution EC enzyme classes (e.g., EC 1.1.1.2).* ***(B)*** *NMDS ordination based on Bray-Curtis dissimilarity of fine-resolution COG classes (e.g., COG1902).*

Figure 4:

Caption: Minewell-enriched functional categories overlap with those induced by experimental TNT exposure

Legend: Functional shifts in minewell microbial communities. ***(A, B)*** *Heatmaps of up- and depleted EC classes and COG categories (DESeq2, FDR < 0.1, $|log_2FC| > 0.6$) comparing minewell and seafloor samples. More classes were depleted than enriched (EC: 35 vs 26; COG: 27 vs 16).* ***(C)*** *Proportion of*

oxidoreductases among enriched and depleted EC classes, showing a higher fraction in enriched classes in minewell samples. ***(D, E)*** *Dot plots comparing environmental functional shifts with a controlled TNT enrichment experiment. In the enrichment experiment, sediment-derived microbial communities were incubated in batch culture with 80 mg L⁻¹ TNT for 12 weeks. The x-axis represents the log_2 fold change of the functional categories in the TNT enrichment relative to its median relative abundance (% assigned reads) across environmental samples, providing a robust baseline for comparison. The y-axis separates functions that are environmentally enriched in minewells relative to seafloor sediments from those that are environmentally depleted . enriched EC and COG classes in minewell samples were more likely to exhibit positive fold changes under TNT exposure than depleted classes.*

Figure 5:

Caption: Variance-based ranking identifies enzyme classes with subtle, TNT-associated enrichment in minewell sediments

Legend: Enzyme classes were ranked by the variance of DESeq2-normalized counts and assessed for higher abundance in minewell compared to seafloor samples. All comparisons include the TNT enrichment dataset. Green points represent the functional profile from the enrichment experiment, in which sediment-derived microbial communities were incubated in batch culture with 80 mg L⁻¹ TNT for 12 weeks. ***(A)*** *Cleveland-style dot plot (% Assigned reads) showing four enzyme classes within the top 50 highest-variance EC categories that are linked to TNT degradation.****(B)*** *Cleveland-style dot plot (% Assigned reads) showing three enzyme classes within the top 50 highest-variance COG categories that are linked to TNT degradation.* ***(C,D)*** *Cleveland-style dot plot (% Assigned reads) for nitroreductase (EC 1.7.1.16; COG0778) and Old Yellow Enzyme families (EC 1.6.99.1; COG1902). Although these functions were not part of the high-variance set, they are included due to their well-established roles in TNT degradation.*

Figure 6:

Caption: MAGs from a TNT-enrichment culture map preferentially onto minewell communities and encode nitrotoluene degradation pathways

Legend: Abundance, environmental distribution, and functional potential of MAGs associated with TNT transformation. ***(A)*** *Relative abundance (%) of metagenome-assembled genomes (MAGs) in the TNT-enriched sample, classified at the species level using GTDB-Tk. The community is composed entirely of Proteobacteria and is dominated by Alloalcanivorax xenomutans (32.1%) and Neptuniibacter pectenicula (28.0%).* ***(B)*** *Cleveland-style dot plot (% mapped reads) of MAGs in minewell and seafloor samples. Environmental reads were mapped to enrichment-derived MAG contigs to assess their in situ abundance. Several MAGs were more abundant in minewells, including Marinobacter alexandrii, Roseovarius lutimaris, and Sulfitobacter pontiacus, with only Marinobacter showing a significant difference (Mann–Whitney, $p < 0.05$).* ***(C)*** *Heatmap showing the number of genes of each MAG assigned to specific xenobiotic degradation pathways based on BlastKOALA annotations. The nitrotoluene degradation pathway is highlighted in bold.*

Figure 7:

Caption: 3D model of the UC-30 wreck and sampling site distribution

Legend: 3D model (by Aarhus University) of the UC-30 wreck based on multibeam sonar data acquired in June 2020 by Aarhus University. Sampling sites at the mine wells (M1-M6) (proximal samples), the seafloor (sf) near the wreck (7 distal samples, SF1-SF7) and the seafloor at 10 m distance (1 distal sample, SF8) are indicated with circles.

Table 1: TNT, its metabolites (4-ADNT, 2-ADNT) and byproducts (2,4-DNT, 1,3-DNB) measured in minewell (M) and seafloor (sf) samples show the spreading of TNT contamination.

Minewell	**TNT (µg/kg)**	**4-ADNT (µg/kg)**	**2-ADNT (µg/kg)**	**2,4-DNT (µg/kg)**	**1,3-DNB (µg/kg)**
UC30 M2	8.939	3.454	2.308	0.018	0.010
UC30 M3	8.560	2.781	1.616	0.011	<0.010*
UC30 M4	0.625	2.908	1.080	0.009	<0.010*
UC30 M5	0.378	0.748	0.437	0.005	0.011
UC30 M6	0.144	0.752	0.246	<0.02*	<0.010*
Seafloor					
UC30 sf1	0.010	0.010	0.008	<0.002*	<0.010*

UC30 sf2	0.012	0.013	0.009	<0.002*	<0.010*
UC30 sf3	0.006	0.015	0.008	<0.002*	<0.010*
UC30 sf4	0.008	0.028	0.009	<0.002*	<0.010*
UC30 sf5	0.007	0.010	0.005	<0.002*	<0.010*
UC30 sf6	0.011	0.017	0.010	<0.002*	<0.010*
UC30 sf7	0.009	0.011	0.007	<0.002*	<0.010*
UC30 sf8a	0.046	0.170	0.112	<0.002*	<0.010*
UC30 sf8b	0.015	0.099	0.045	<0.002*	<0.010*

***Compound was below limit of detection**

A

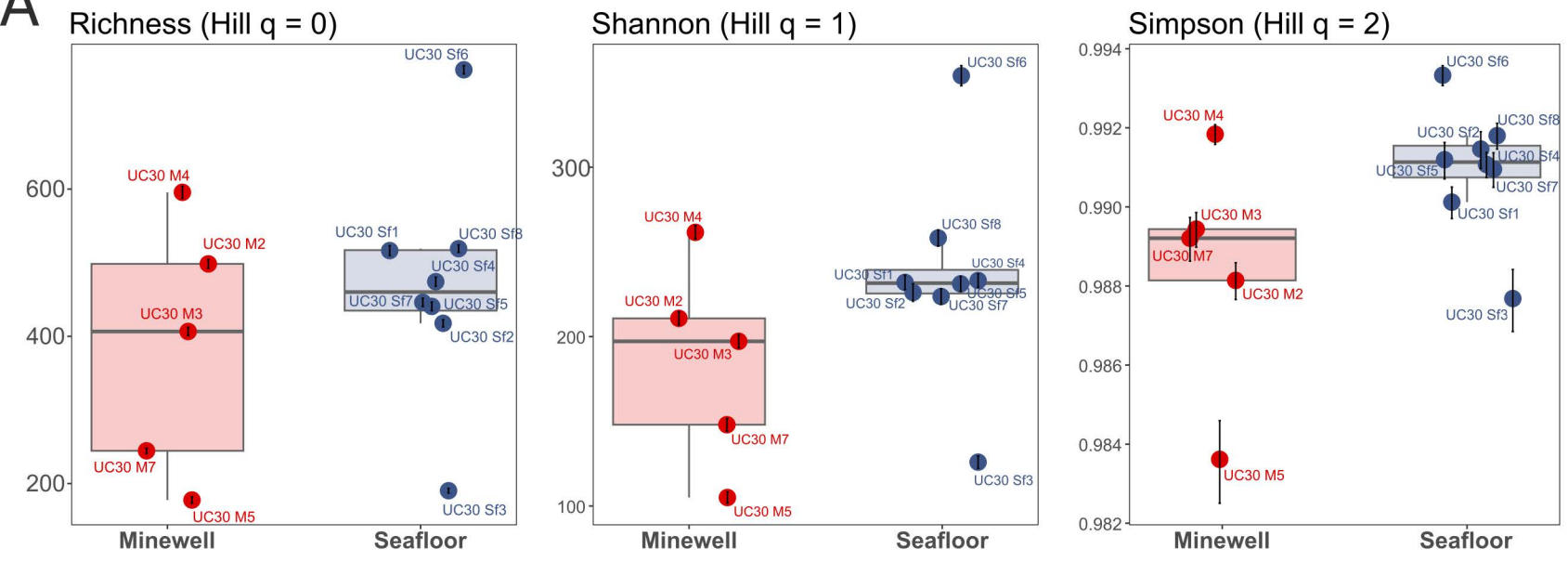

Sampling location Minewell Seafloor

B

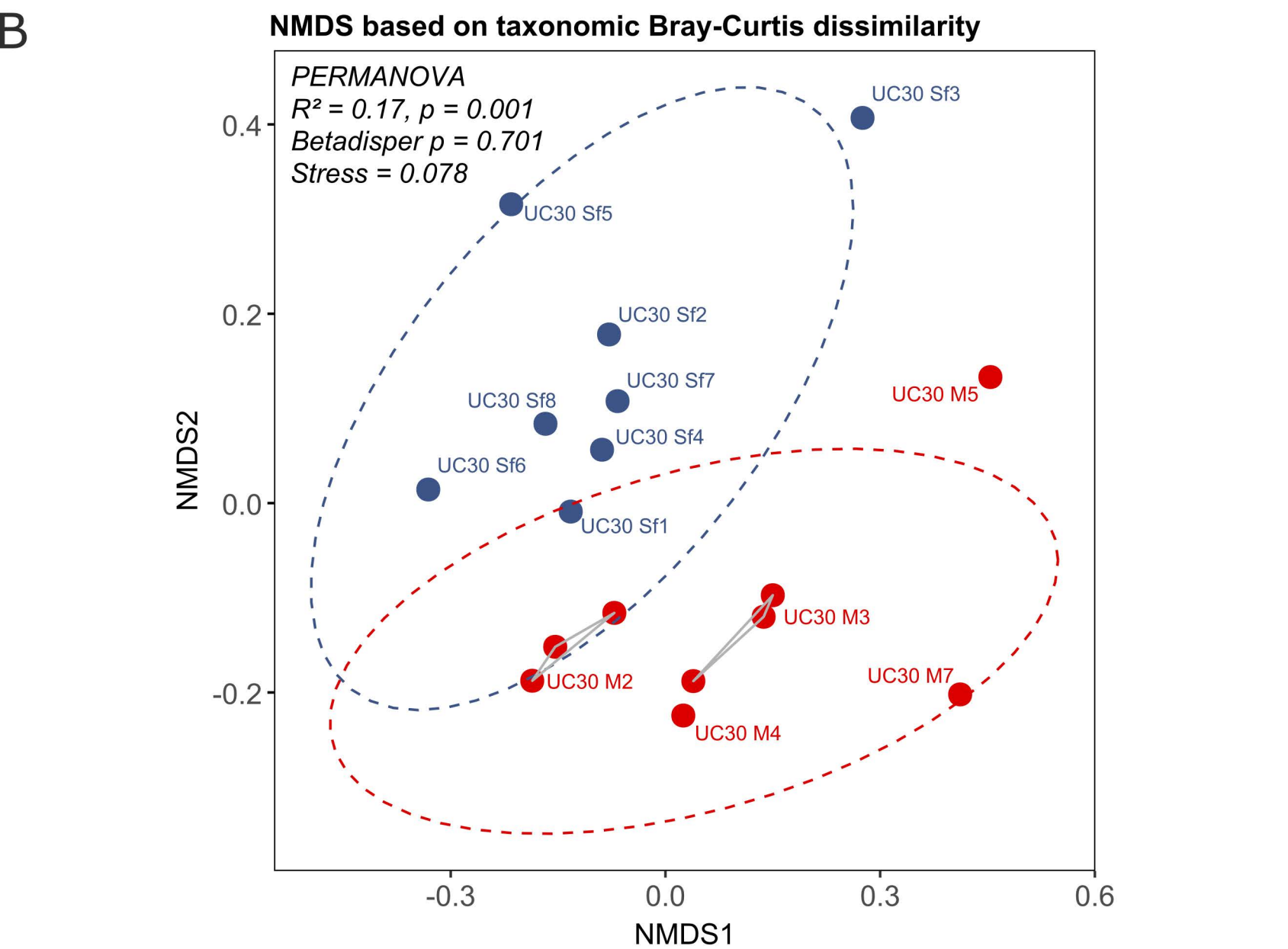

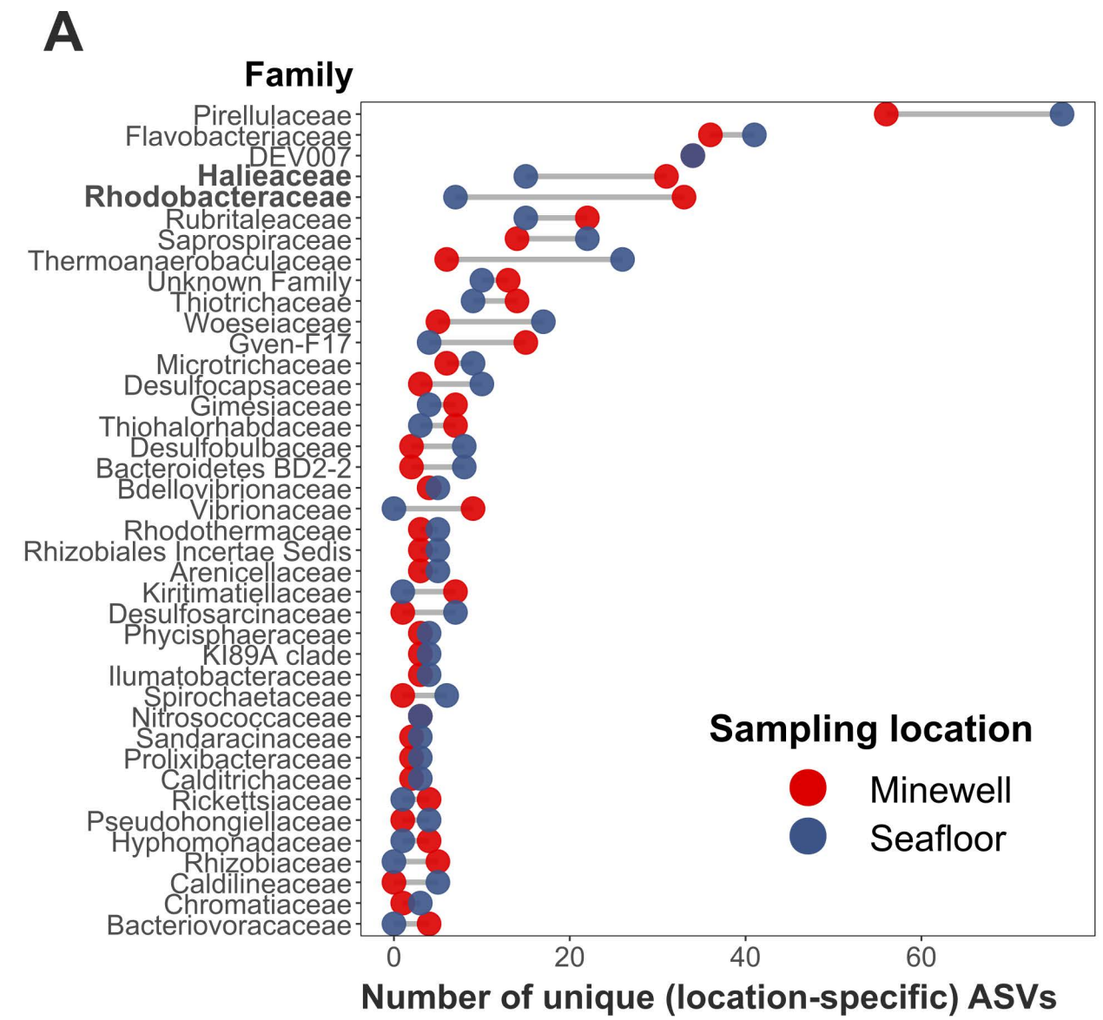
A
Family
Pirellulaceae
Flavobacteriaceae
DEV007
Halieaceae
Rhodobacteraceae
Rubritaleaceae
Saprospiraceae
Thermoanaerobaculaceae
Unknown Family
Thiotrichaceae
Woeseiaceae
Gven-F17
Microtrichaceae
Desulfocapsaceae
Gimesiaceae
Thiohalorhabdaceae
Desulfobulbaceae
Bacteroidetes BD2-2
Bdellovibrionaceae
Vibrionaceae
Rhodothermaceae
Rhizobiales Incertae Sedis
Arenicellaceae
Kiritimatiellaceae
Desulfosarcinaceae
Phycisphaeraceae
KI89A clade
Ilumatobacteraceae
Spirochaetaceae
Nitrosococcaceae
Sandaracinaceae
Prolixibacteraceae
Calditrichaceae
Rickettsiaceae
Pseudohongiellaceae
Hyphomonadaceae
Rhizobiaceae
Caldilineaceae
Chromatiaceae
Bacteriovoracaceae
Sampling location
Minewell
Seafloor
0
20
40
60
Number of unique (location-specific) ASVs

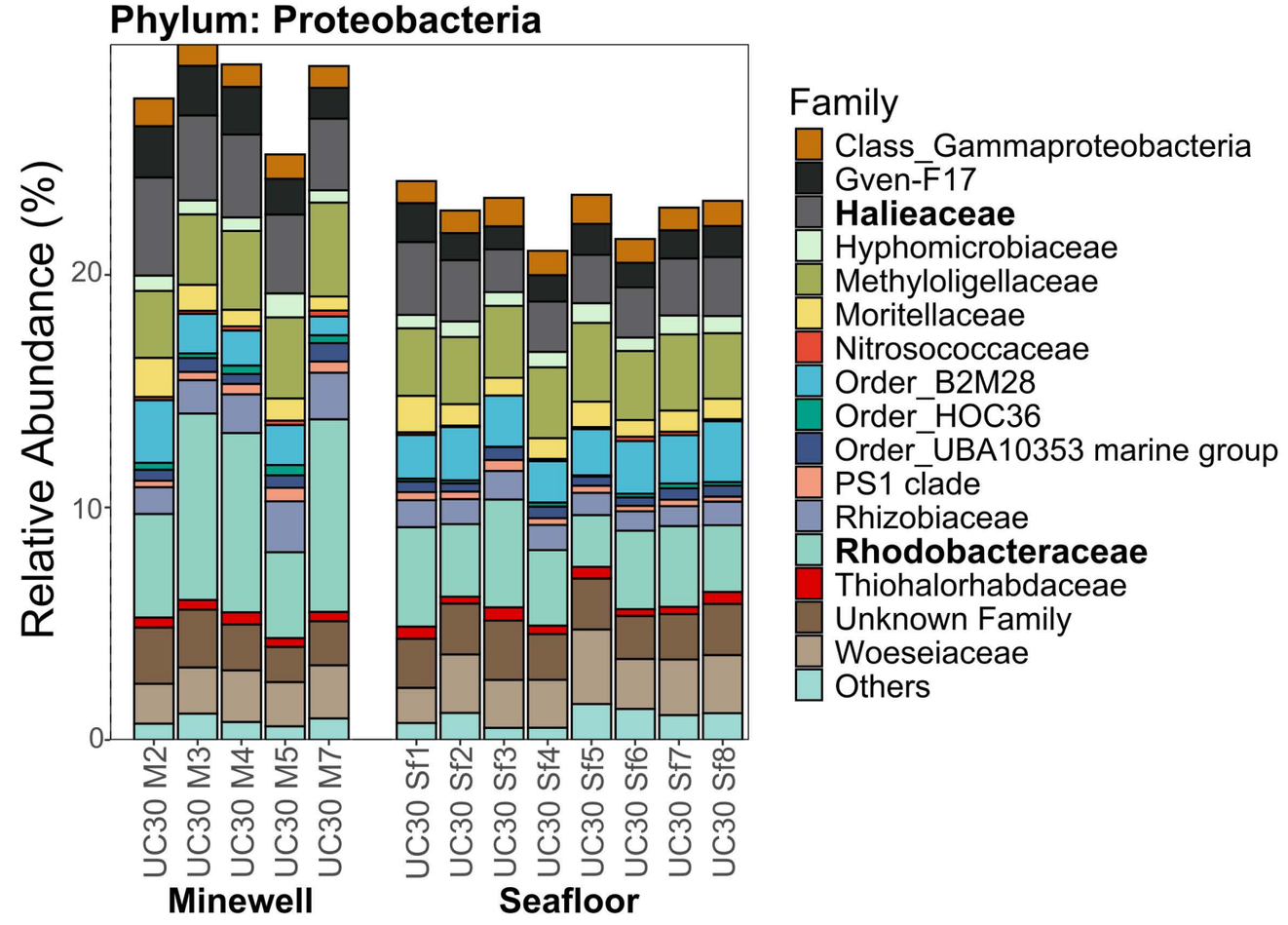
B
Phylum: Proteobacteria
Relative Abundance (%)
0
10
20
UC30 M2
UC30 M3
UC30 M4
UC30 M5
UC30 M7
UC30 Sf1
UC30 Sf2
UC30 Sf3
UC30 Sf4
UC30 Sf5
UC30 Sf6
UC30 Sf7
UC30 Sf8
Minewell
Seafloor
Family
Class_Gammaproteobacteria
Gven-F17
Halieaceae
Hyphomicrobiaceae
Methyloligellaceae
Moritellaceae
Nitrosococcaceae
Order_B2M28
Order_HOC36
Order_UBA10353 marine group
PS1 clade
Rhizobiaceae
Rhodobacteraceae
Thiohalorhabdaceae
Unknown Family
Woeseiaceae
Others

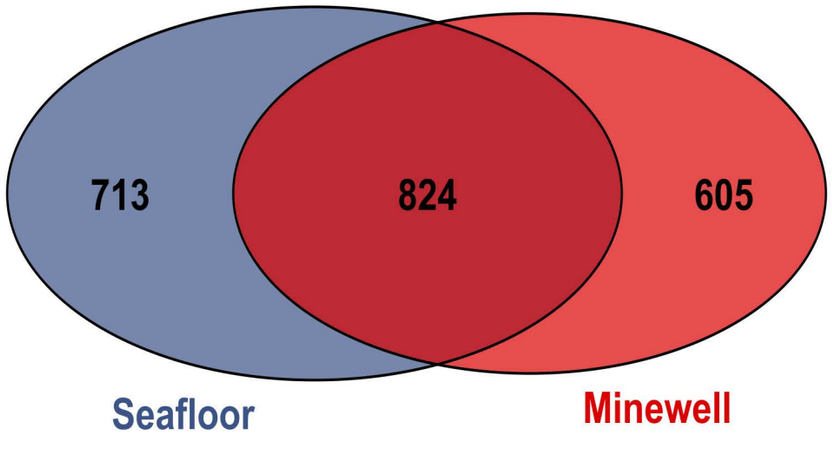
C
Minewell vs. Seafloor ASVs
713
824
605
Seafloor
Minewell

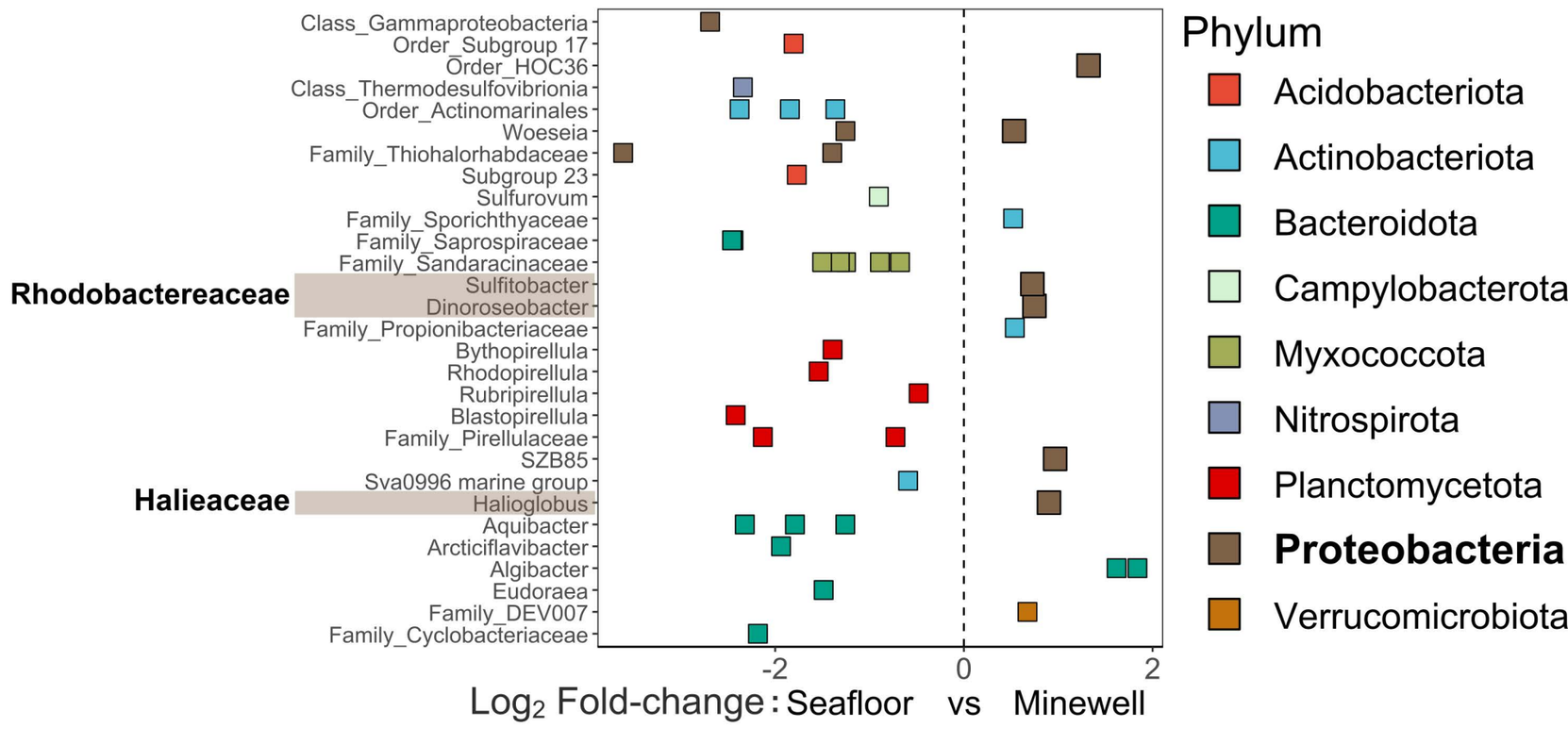
D
Class_Gammaproteobacteria
Order_Subgroup 17
Order_HOC36
Class_Thermodesulfovibrionia
Order_Actinomarinales
Woeseia
Family_Thiohalorhabdaceae
Subgroup 23
Sulfurovum
Family_Sporichthyaceae
Family_Saprospiraceae
Family_Sandaracinaceae
Rhodobactereaceae
Sulfitobacter
Dinoroseobacter
Family_Propionibacteriaceae
Bythopirellula
Rhodopirellula
Rubripirellula
Blastopirellula
Family_Pirellulaceae
SZB85
Sva0996 marine group
Halieaceae
Halioglobus
Aquibacter
Arcticiflavibacter
Algibacter
Eudoraea
Family_DEV007
Family_Cyclobacteriaceae
-2
0
2
Log2 Fold-change : Seafloor vs Minewell
Phylum
Acidobacteriota
Actinobacteriota
Bacteroidota
Campylobacterota
Myxococcota
Nitrospirota
Planctomycetota
Proteobacteria
Verrucomicrobiota

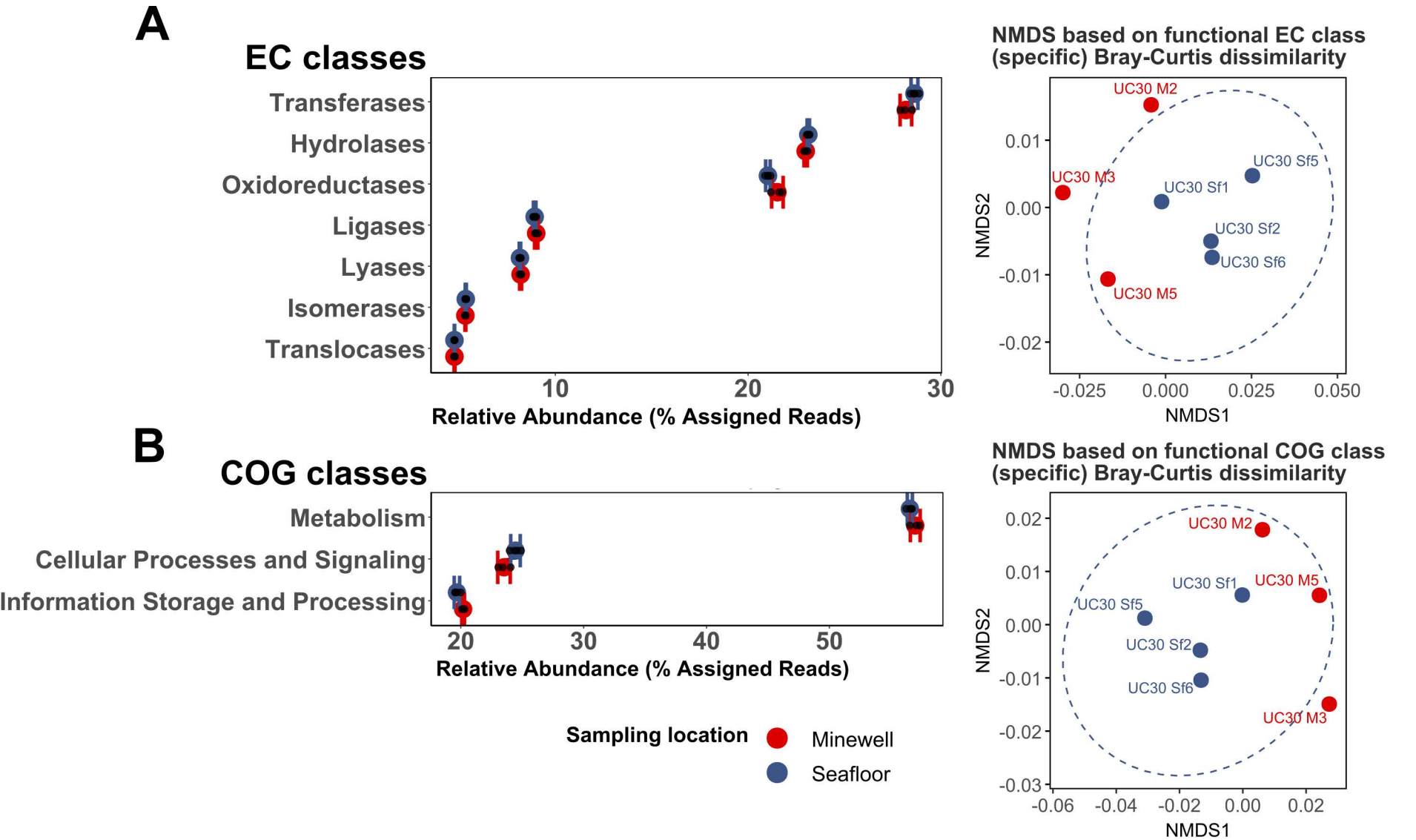
A
EC classes
Transferases
Hydrolases
Oxidoreductases
Ligases
Lyases
Isomerases
Translocases
10
20
30
Relative Abundance (% Assigned Reads)
NMDS based on functional EC class (specific) Bray-Curtis dissimilarity
UC30 M2
UC30 M3
UC30 Sf5
UC30 Sf1
UC30 Sf2
UC30 Sf6
UC30 M5
0.01
0.00
-0.01
-0.02
NMDS2
-0.025
0.000
0.025
0.050
NMDS1
B
COG classes
Metabolism
Cellular Processes and Signaling
Information Storage and Processing
20
30
40
50
Relative Abundance (% Assigned Reads)
NMDS based on functional COG class (specific) Bray-Curtis dissimilarity
UC30 M2
UC30 Sf1
UC30 M5
UC30 Sf5
UC30 Sf2
UC30 Sf6
UC30 M3
0.02
0.01
0.00
-0.01
-0.02
-0.03
NMDS2
-0.06
-0.04
-0.02
0.00
0.02
NMDS1
Sampling location
Minewell
Seafloor

A

Differentially abundant Enzyme COG Classes

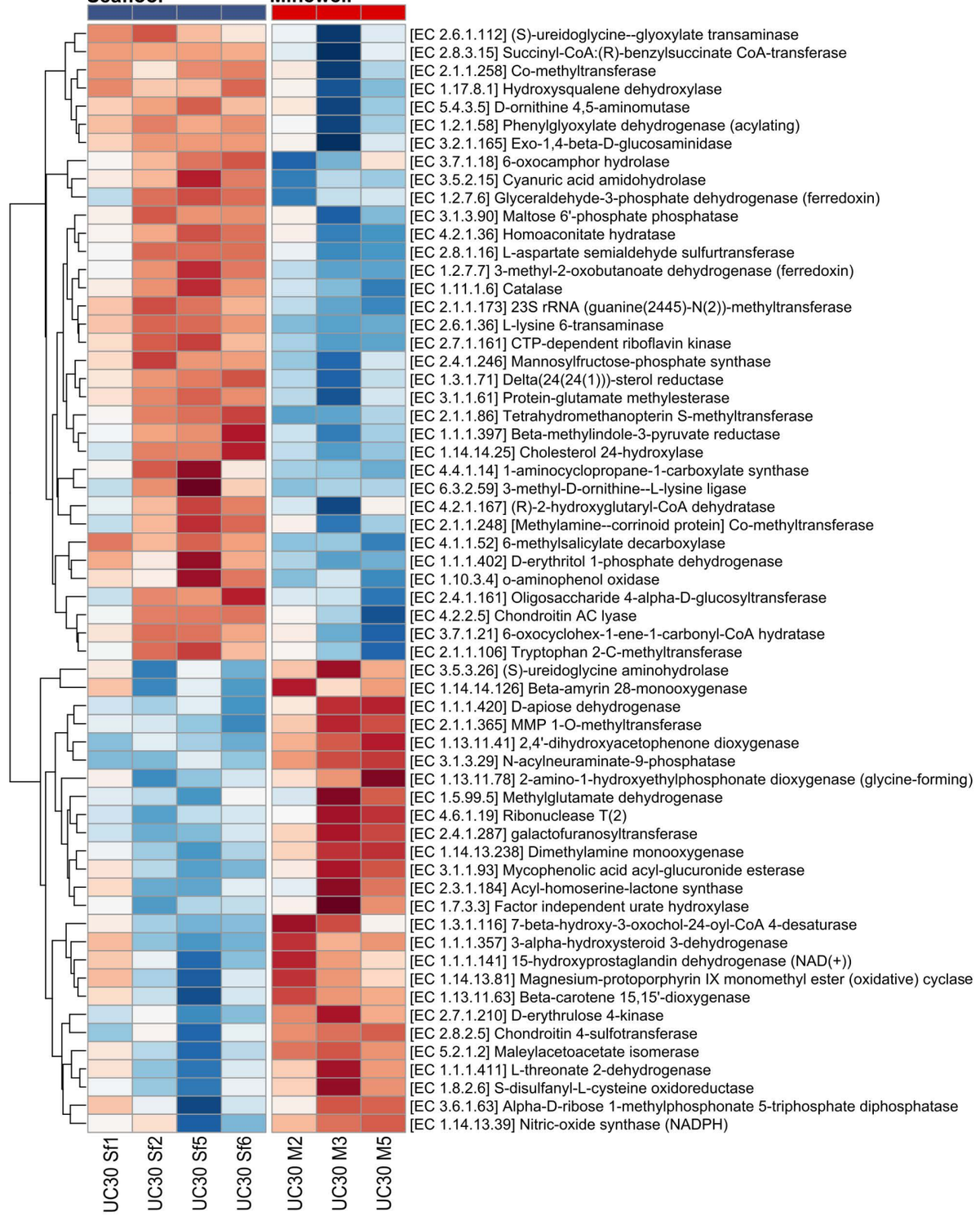

B

Differentially abundant Enzyme EC Classes

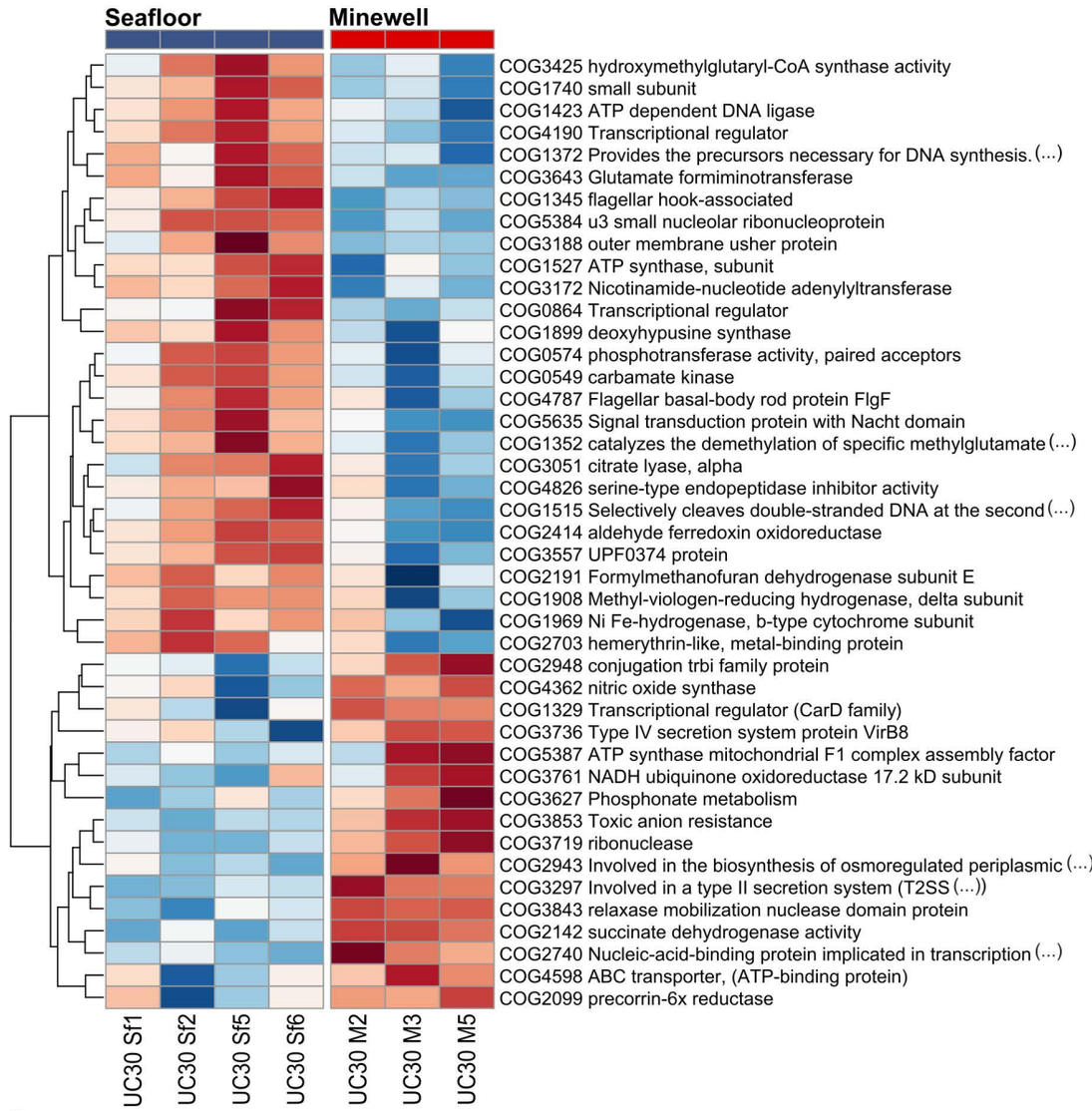

C

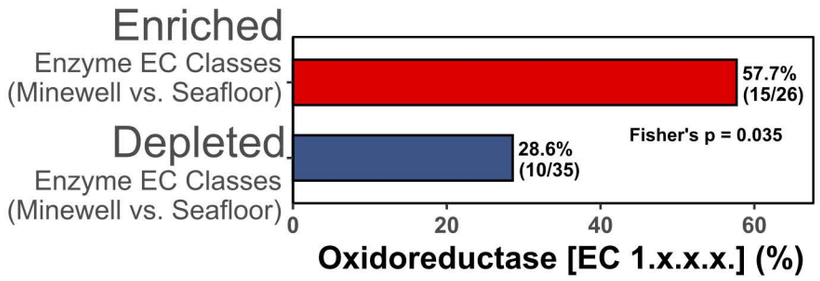

D

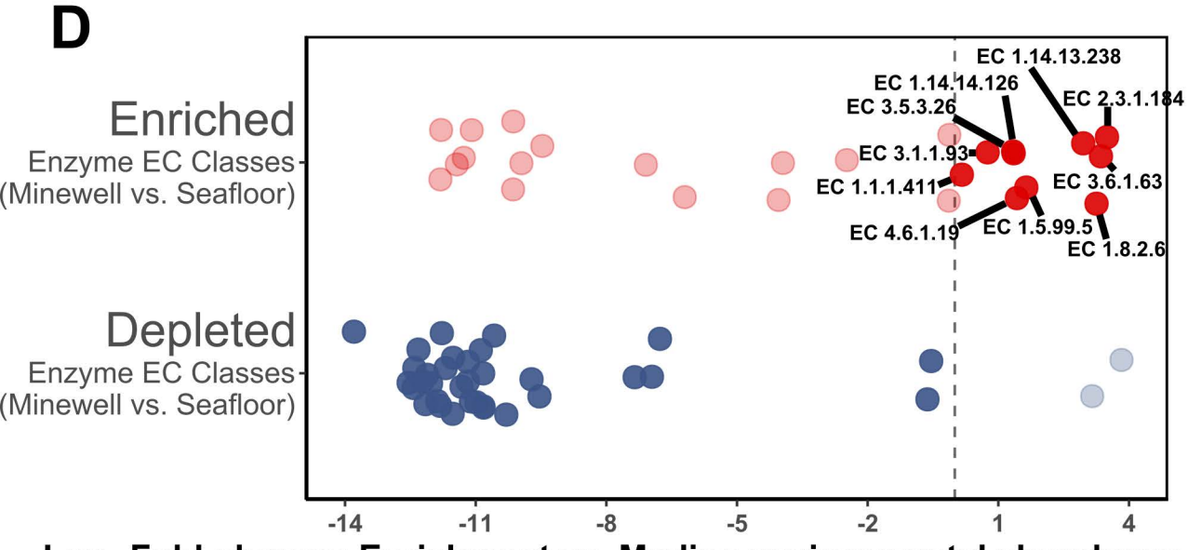

E

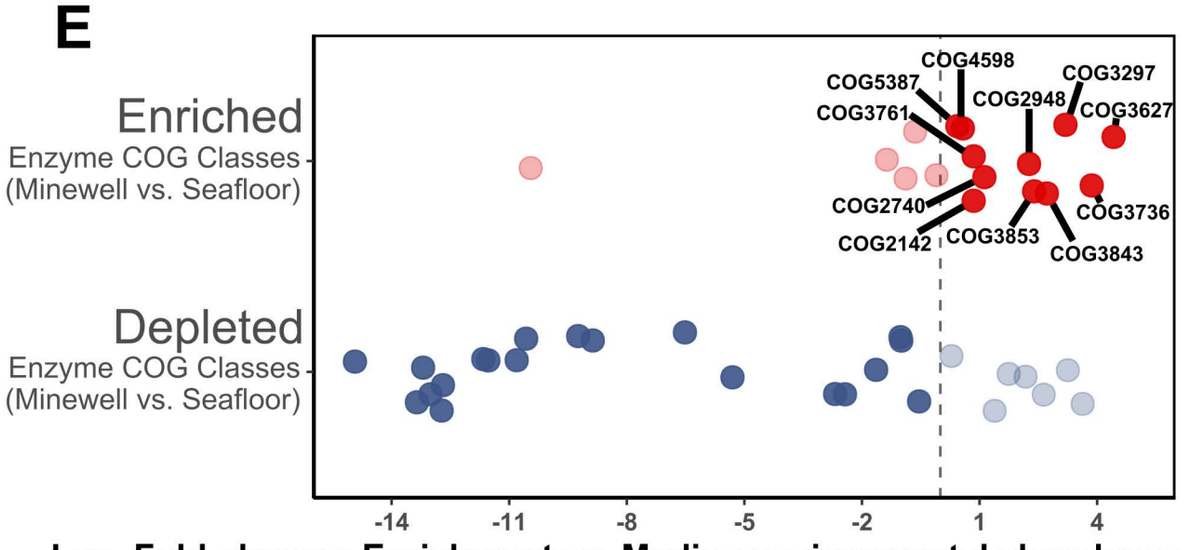

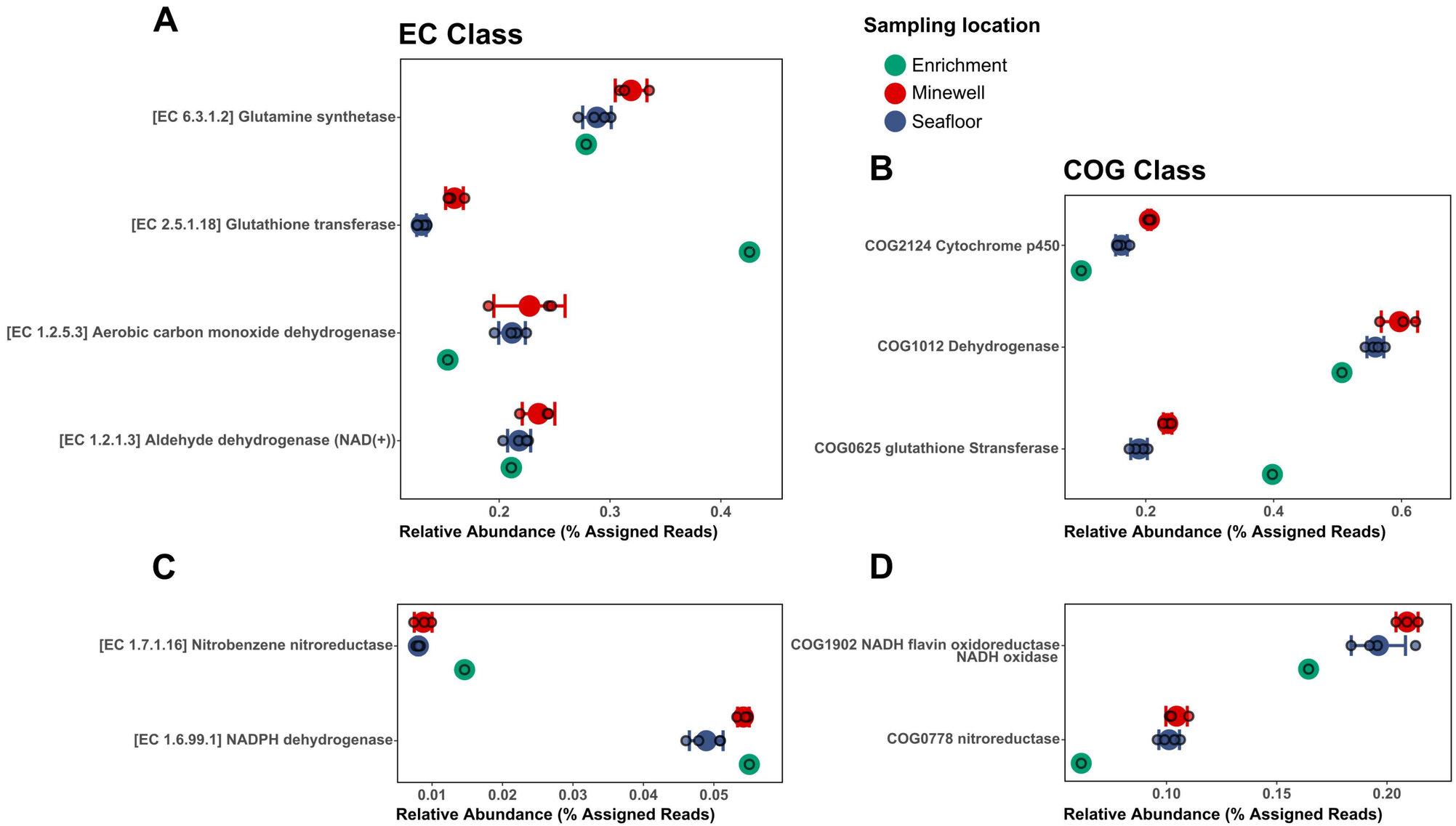
A
EC Class
[EC 6.3.1.2] Glutamine synthetase
[EC 2.5.1.18] Glutathione transferase
[EC 1.2.5.3] Aerobic carbon monoxide dehydrogenase
[EC 1.2.1.3] Aldehyde dehydrogenase (NAD(+))
0.2
0.3
0.4
Relative Abundance (% Assigned Reads)
Sampling location
Enrichment
Minewell
Seafloor
B
COG Class
COG2124 Cytochrome p450
COG1012 Dehydrogenase
COG0625 glutathione Stransferase
0.2
0.4
0.6
Relative Abundance (% Assigned Reads)
C
[EC 1.7.1.16] Nitrobenzene nitroreductase
[EC 1.6.99.1] NADPH dehydrogenase
0.01
0.02
0.03
0.04
0.05
Relative Abundance (% Assigned Reads)
D
COG1902 NADH flavin oxidoreductase NADH oxidase
COG0778 nitroreductase
0.10
0.15
0.20
Relative Abundance (% Assigned Reads)

A

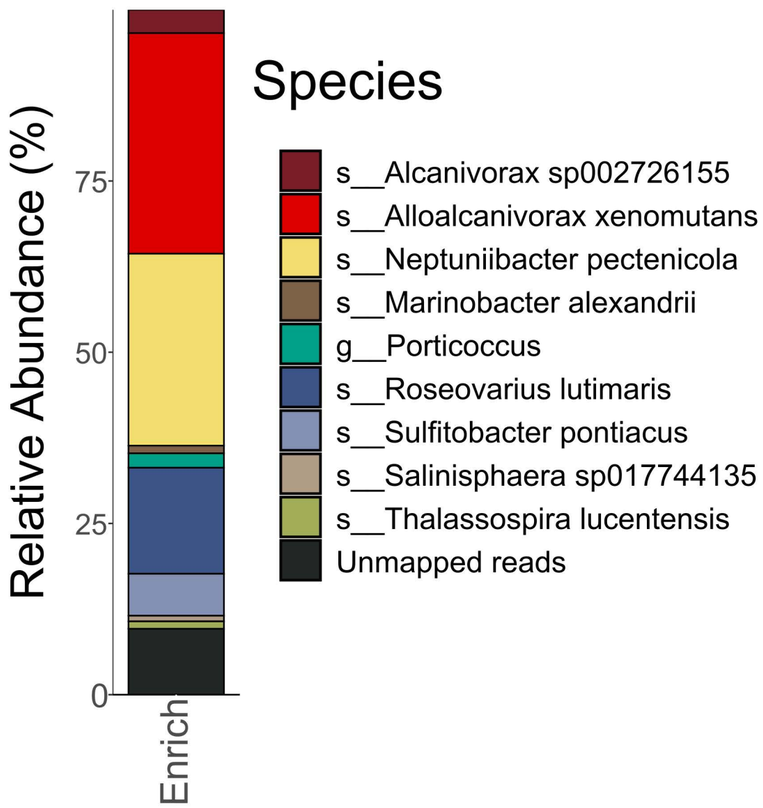
Relative Abundance (%)
75
50
25
0
Enrich
Species
s__Alcanivorax sp002726155
s__Alloalcanivorax xenomutans
s__Neptuniibacter pectenicola
s__Marinobacter alexandrii
g__Porticoccus
s__Roseovarius lutimaris
s__Sulfitobacter pontiacus
s__Salinisphaera sp017744135
s__Thalassospira lucentensis
Unmapped reads

B

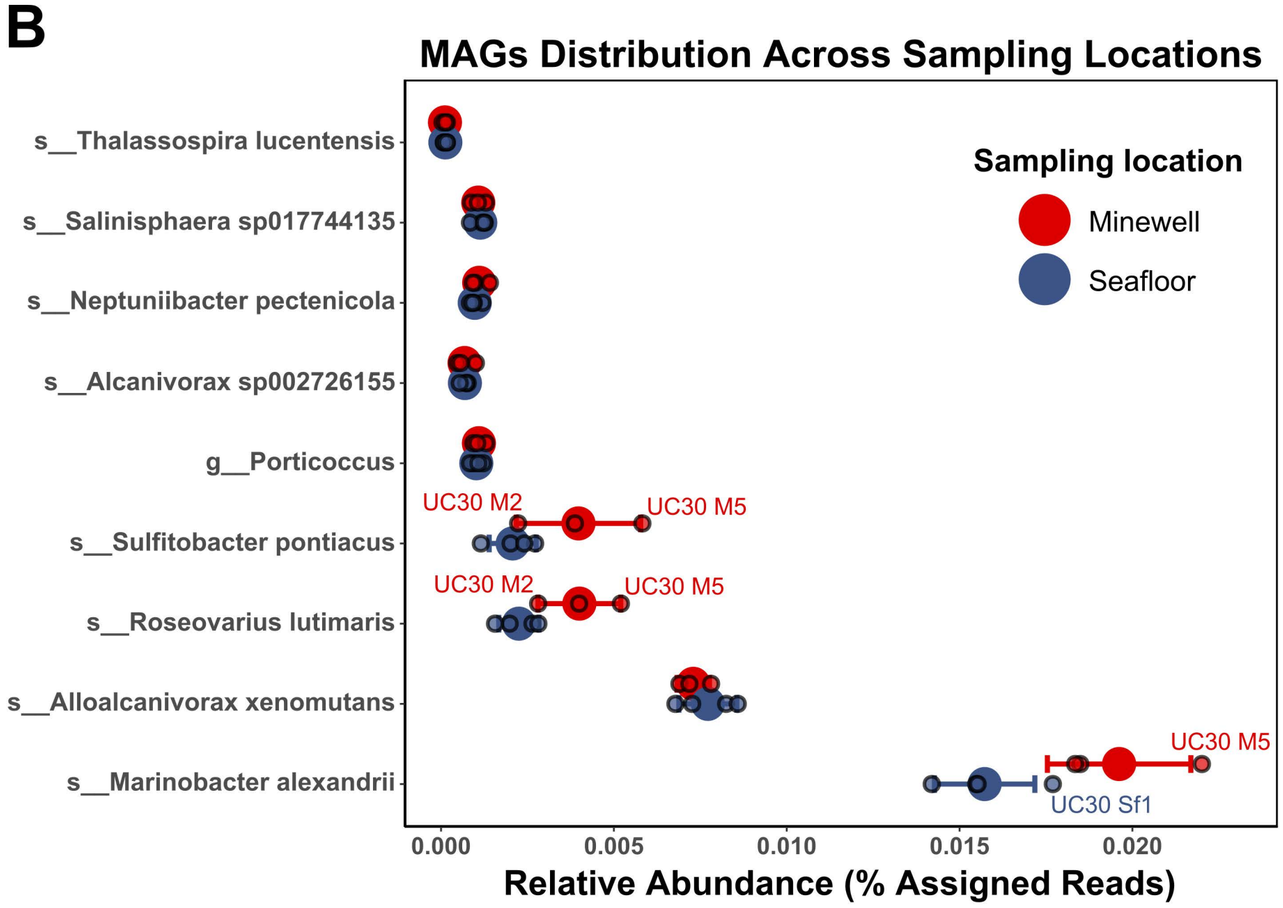
MAGs Distribution Across Sampling Locations
s__Thalassospira lucentensis
s__Salinisphaera sp017744135
s__Neptuniibacter pectenicola
s__Alcanivorax sp002726155
g__Porticoccus
s__Sulfitobacter pontiacus
s__Roseovarius lutimaris
s__Alloalcanivorax xenomutans
s__Marinobacter alexandrii
Sampling location
Minewell
Seafloor
UC30 M2
UC30 M5
UC30 M2
UC30 M5
UC30 M5
UC30 Sf1
0.000
0.005
0.010
0.015
0.020
Relative Abundance (% Assigned Reads)

C

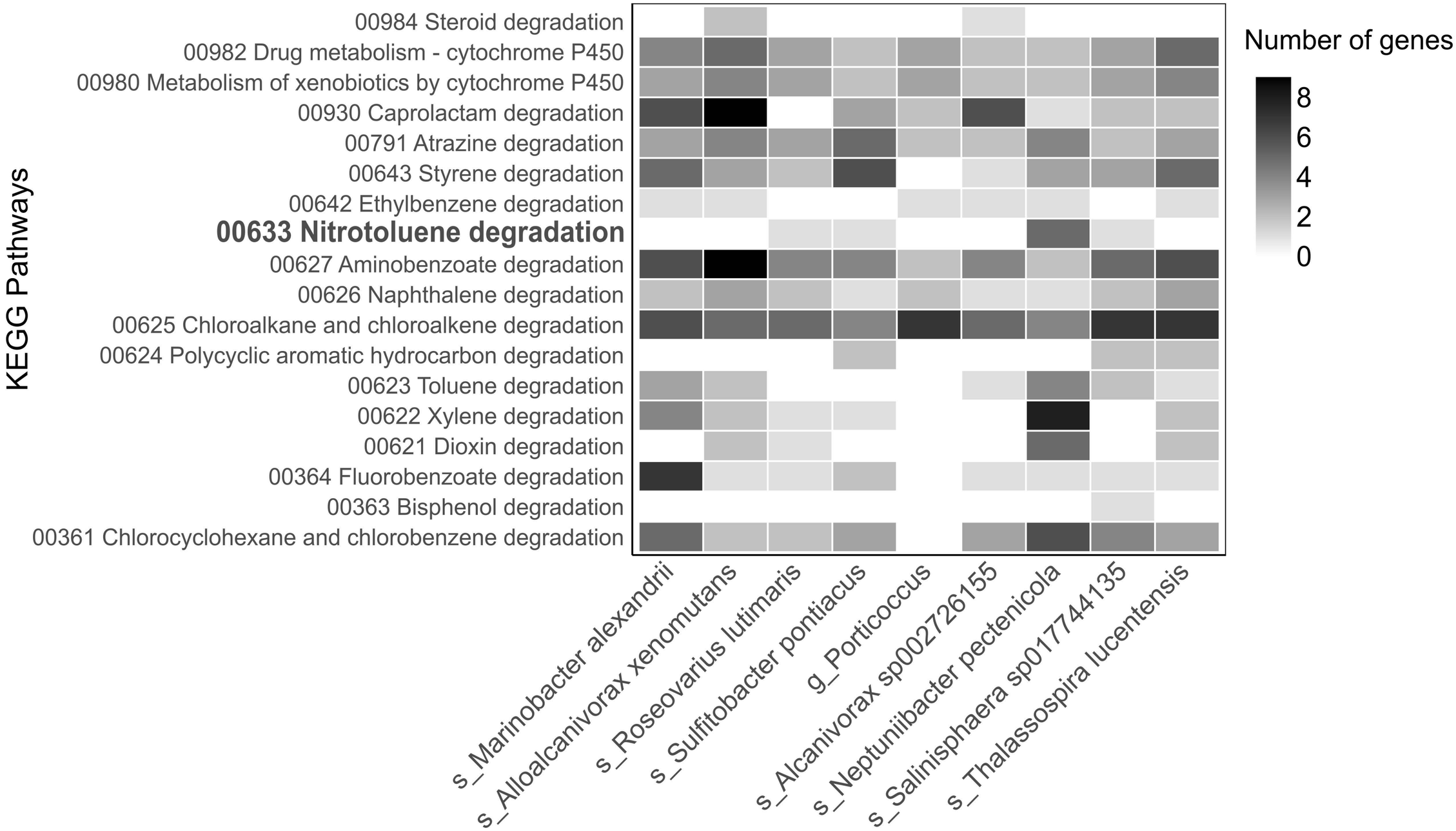
KEGG Pathways
00984 Steroid degradation
00982 Drug metabolism - cytochrome P450
00980 Metabolism of xenobiotics by cytochrome P450
00930 Caprolactam degradation
00791 Atrazine degradation
00643 Styrene degradation
00642 Ethylbenzene degradation
00633 Nitrotoluene degradation
00627 Aminobenzoate degradation
00626 Naphthalene degradation
00625 Chloroalkane and chloroalkene degradation
00624 Polycyclic aromatic hydrocarbon degradation
00623 Toluene degradation
00622 Xylene degradation
00621 Dioxin degradation
00364 Fluorobenzoate degradation
00363 Bisphenol degradation
00361 Chlorocyclohexane and chlorobenzene degradation
s_Marinobacter alexandrii
s_Alloalcanivorax xenomutans
s_Roseovarius lutimaris
s_Sulfitobacter pontiacus
g_Porticoccus
s_Alcanivorax sp002726155
s_Neptuniibacter pectenicola
s_Salinisphaera sp017744135
s_Thalassospira lucentensis
Number of genes
8
6
4
2
0

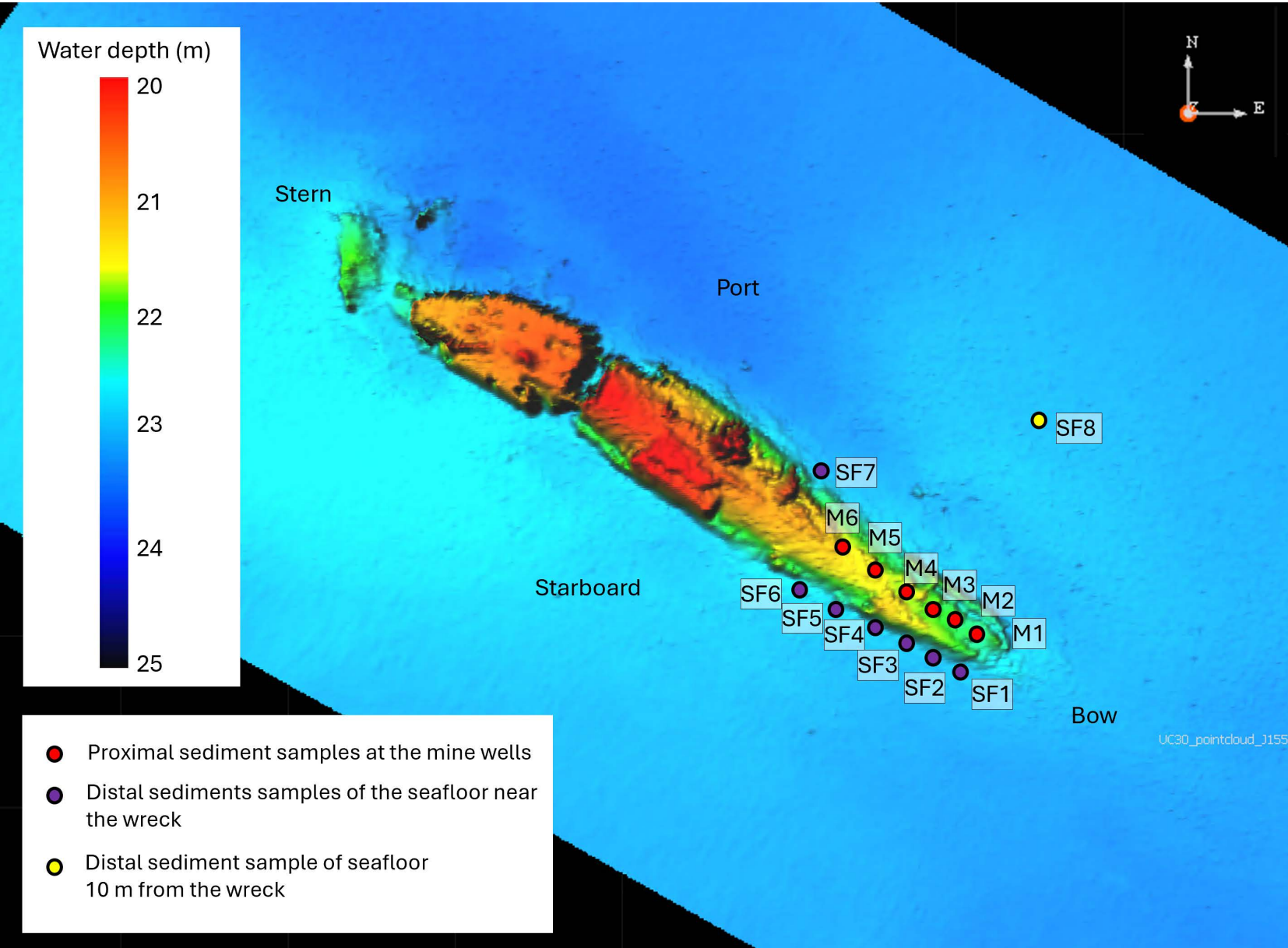
Water depth (m)
20
21
22
23
24
25
N
E
Stern
Port
Starboard
Bow
SF8
SF7
M6
M5
M4
M3
M2
M1
SF6
SF5
SF4
SF3
SF2
SF1
Proximal sediment samples at the mine wells
Distal sediments samples of the seafloor near the wreck
Distal sediment sample of seafloor 10 m from the wreck
UC30_pointcloud_J155